

RECEIVED
OCT 10 1995
OSTI

**Tank Waste Treatment Science
Task Quarterly Report for
October - December 1994**

J. P. LaFemina (Task Leader)

January 1995

**Prepared for the U.S. Department of Energy
under Contract DE-AC06-76RLO 1830**

**Pacific Northwest Laboratory
Operated for the U.S. Department of Energy
by Battelle Memorial Institute**



DISCLAIMER

This report was prepared as an account of work sponsored by an agency of the United States Government. Neither the United States Government nor any agency thereof, nor Battelle Memorial Institute, nor any of their employees, makes any warranty, express or implied, or assumes any legal liability or responsibility for the accuracy, completeness, or usefulness of any information, apparatus, product, or process disclosed, or represents that its use would not infringe privately owned rights. Reference herein to any specific commercial product, process, or service by trade name, trademark, manufacturer, or otherwise does not necessarily constitute or imply its endorsement, recommendation, or favoring by the United States Government or any agency thereof, or Battelle Memorial Institute. The views and opinions of authors expressed herein do not necessarily state or reflect those of the United States Government or any agency thereof.

PACIFIC NORTHWEST LABORATORY
operated by
BATTELLE MEMORIAL INSTITUTE
for the
UNITED STATES DEPARTMENT OF ENERGY
under Contract DE-AC06-76RLO 1830



This document was printed on recycled paper.

DISCLAIMER

Portions of this document may be illegible in electronic image products. Images are produced from the best available original document.

**Tank Waste Treatment Science Task
Quarterly Report for
October - December 1994**

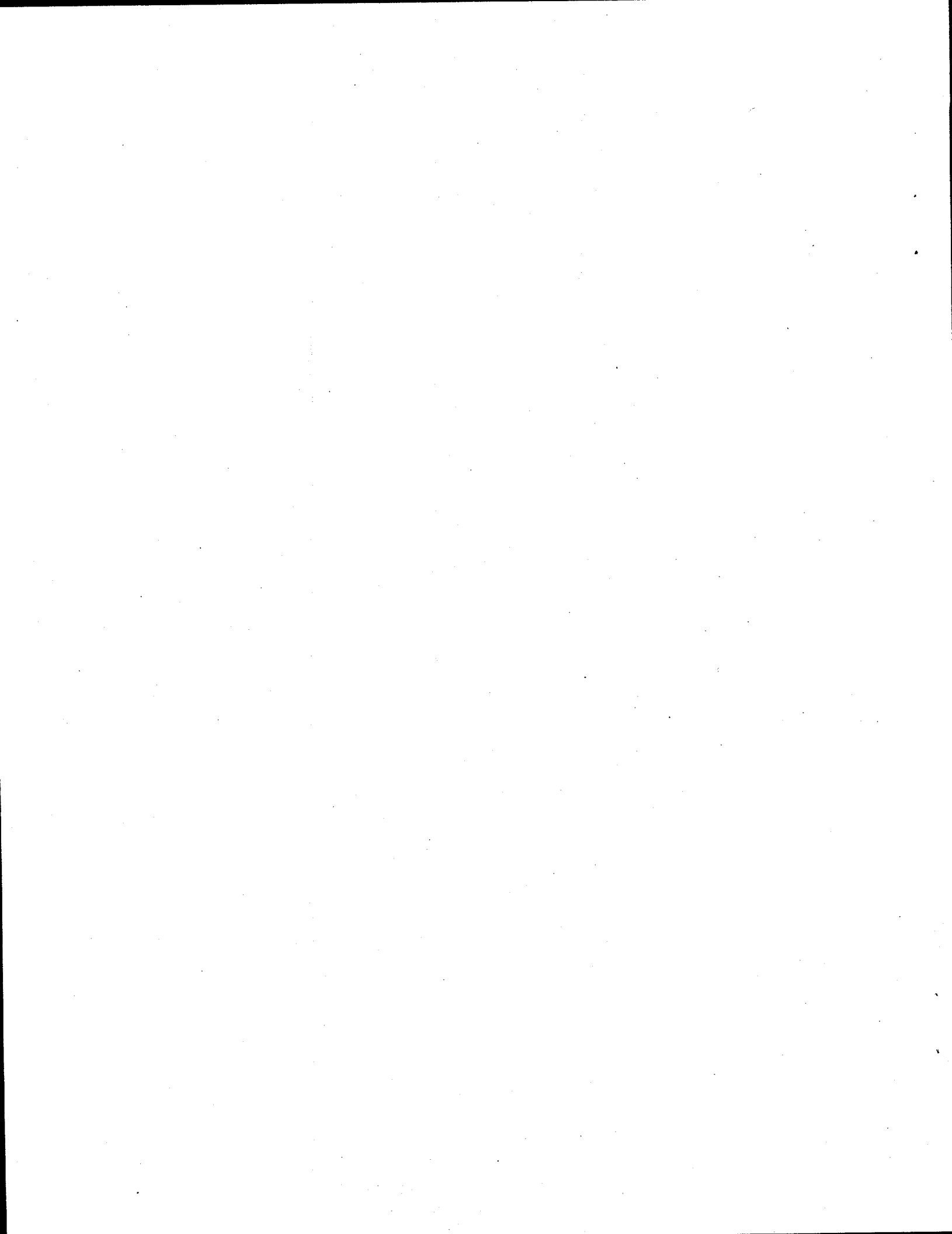
J. P. LaFemina (Task Leader)

G. S. Anderson	J. G. Hill
D. L. Blanchard	E. A. Jenne
P. J. Bruinsma	M. M. Lamoureux
B. C. Bunker	J. Liu
N. G. Colton	B. M. Rapko
S. D. Conradson	D. R. Rector
J. L. Cox	P. A. Smith
J. Craig Hutton	L. Song
A. R. Felmy	D. L. Styris
R. L. Gordon	L. E. Thomas
G. L. Graff	A. J. Villegas
N. J. Hess	Y. Wang

January 1995

Prepared for
the U.S. Department of Energy
under Contract DE-AC06-76RLO 1830

Pacific Northwest Laboratory
Richland, Washington 99352



Summary

This report describes the work performed by Pacific Northwest Laboratory (PNL) during the first quarter of FY 1995 (October - December 1994) under the Tank Waste Treatment Science Task of the Tank Waste Remediation System (TWRS) Pretreatment Technology Development Project. Work was performed in the following areas: 1) analytical methods development, 2) sludge dissolution modeling, 3) sludge characterization studies, 4) sludge component speciation, 5) pretreatment chemistry evaluation, and 6) colloidal studies for solid-liquid separations. Significant accomplishments are highlighted below:

- Installation and testing of a particle size analysis system and a capillary ion analyzer.
- Testing the existing thermodynamic model for the major electrolyte components of tank wastes by comparing predicted solubilities of NaNO_3 and NaNO_2 in simulated waste with direct experimental observations.
- Submission of three papers for publication in the ACS Symposium Series on Scientific Issues Related to Safety and Treatment of Hanford Wastes.
- Presentation of a seminar entitled "Speciation of Sr and Ni in Tanks C-112 and C-109 Sludges."
- Fabrication (Los Alamos National Laboratory) of eight sample holders and two sample assemblies from a corrosion-resistant alloy for x-ray absorption spectroscopy experiments performed in March 1995 at the Stanford Synchrotron Radiation Laboratory.
- Development of the data structure for the statistical analysis of physical and rheological tank waste properties using the Sort on Radioactive Waste Type (SORWT) methodology.
- Obtaining and structuring the "Braun database" that contains records of historical analytical data for evaluation with the SORWT model to provide a tank-by-tank estimate of analyte concentrations.
- Preparation and characterization of colloidal suspensions of boehmite (AlOOH) and gibbsite [$\text{Al}(\text{OH})_3$], in terms of primary particle size and shape, surface charge, and degree of agglomeration. While it is too early to draw definitive conclusions, the work performed to date suggests the following information about current guidelines.
 1. It appears that many of the current guidelines used in evaluating the baseline processes for solid-liquid separations are valid if the primary particles in sludge are larger than $10 \mu\text{m}$ in size. With large particles it is possible to achieve low slurry viscosities ($< 60 \text{ cp}$) at high solids loadings ($> 10 \text{ vol}\%$) for retrieval and transport, to have reasonable initial sedimentation velocities ($> 3 \text{ cm/hr}$) for settle-decant operations, and to achieve rapid filtration rates ($> 1 \text{ cm/hr}$).

2. The current processing guidelines do not appear to be valid if the bulk of the material to be processed consists of submicron particles. Fine colloidal particles can form highly viscous ($> 25,000$ cp) shear-thinning liquids at solids loadings as low as 3 vol%, can form suspensions that exhibit negligible sedimentation velocities (either in the form of highly dispersed suspensions or as highly agglomerated gels), and can form impermeable filter cakes that will clog most filtration media.

It is too early to tell the extent to which large particles (or particle mixtures) might mediate the potentially harmful effects of the smaller particles, or what alternatives (involving either chemistry or equipment modifications) might be most effective in controlling desired solid-liquid separations when submicron particles are present.

- Development of computer programs to model the rheological and sedimentation properties of colloidal suspensions.
- Identification of space requirements and equipment for the Hot Colloids Laboratory.

Contents

Summary	iii
1.0 Introduction	1.1
2.0 Analytical Methods Development	2.1
2.1 Particle Size Analysis System	2.1
2.2 Capillary Ion Analyzer	2.2
2.3 Reference	2.3
3.0 Sludge Dissolution Modeling	3.1
3.1 Major Electrolyte Studies	3.1
3.1.1 Complete Ongoing Osmotic Studies	3.2
3.1.2 Implement Computer Code Modifications	3.2
3.1.3 Perform Model Validation Calculations	3.2
3.2 Alkaline Earth Cation Inclusion	3.2
3.2.1 Locate/Organize Thermochemical Data	3.2
3.2.2 Identify Subsystems/Interactions for which Data Are Not Available	3.3
3.2.3 Procure Chemicals	3.3
3.3 Actinide Studies	3.4
3.4 Bismuth Studies	3.5
3.5 Kinetic Modeling	3.5
3.6 Publications	3.6
3.7 Reference	3.7
4.0 Sludge Characterization Studies	4.1
5.0 Sludge Component Speciation	5.1
5.1 X-ray Absorption Spectroscopy	5.1
5.1.1 Presentations	5.1
5.1.2 XAS Testing	5.2

Contents (contd)

5.2	Laser Ablation/Mass Spectrometry	5.2
6.0	Pretreatment Chemistry Evaluation	6.1
6.1	Process Chemistry Evaluation	6.1
6.1.1	Silicon	6.1
6.1.2	Aluminum	6.2
6.2	Data Evaluation Using the Sort on Radioactive Waste Type (SORWT) Model	6.3
6.2.1	Evaluation of Physical Properties	6.3
6.2.2	Evaluation of Historical Data Set	6.4
6.3	References	6.4
7.0	Colloidal Studies for Solid-Liquid Separation	7.1
7.1	Experimental Studies	7.2
7.1.1	General Particle Characterization	7.2
7.1.2	Viscosity Measurements	7.8
7.1.3	Sedimentation and Centrifugation	7.12
7.1.4	Pressure Filtration Studies	7.15
7.2	Modeling Studies	7.18
7.2.1	Stokesian Dynamics Model	7.18
7.2.2	Sedimentation Equilibrium Model	7.20
7.3	Hot Colloids Laboratory	7.23
7.4	Summary	7.23
7.5	References	7.24

Figures

3.1	Experimental and Calculated Solubilities of NaNO_3 at 60°C	3.3
3.2	Experimental and Calculated Solubilities of NaNO_3 at 80°C	3.4
3.3	Experimental and Calculated Solubilities of NaNO_2 at 60°C	3.5
3.4	Experimental and Calculated Solubilities of NaNO_2 at 80°C	3.6
7.1	Major Steps in Tank Waste Processing	7.1
7.2	Electrical Double Layers	7.5
7.3	Surface Charge of AlOOH	7.6
7.4	Boehmite (AlOOH) Agglomeration vs. pH	7.7
7.5	Viscosity of Dispersed Boehmite Suspensions	7.8
7.6	Viscosity of Agglomerated Boehmite Suspensions	7.9
7.7	Boehmite Viscosity vs. pH	7.10
7.8	Viscosity vs. Primary Particle Size	7.11
7.9	Viscosity of Boehmite Suspensions vs. Sample History	7.12
7.10	Gibbsite Sedimentation Rates	7.14
7.11	Impact of Agglomeration on Settle-Decant Steps	7.15
7.12	Filtration Rates vs. Time	7.16
7.13	Permeability of Boehmite Filter Cakes	7.17
7.14	Relative Viscosity as a Function of Volume Fraction	7.19
7.15	Relative Sedimenting Velocities of a Cubic Array of Hard Spheres as a Function of Volume Fraction	7.19
7.16	Reduced Density Profile of a Monodispersed Hard Sphere Suspension for $n_s^*=40$ and $a^*=0.2$	7.21

Figures (contd)

7.17	Reduced Density Profile of a Monodispersed Hard Sphere Suspension for $n_s^* = 40$ and $a^* = 0.4$	7.21
7.18	Reduced Density Profile of an Equimolar Binary Hard Sphere Suspension with Particle Size Ratio $\sigma_2/\sigma_1 = 0.5$ and Mass Ratio $m_1/m_2 = (\sigma_1/\sigma_2)^3$ (equal density)	7.22
7.19	Reduced Density Profile of an Equimolar Binary Hard Sphere Suspension with Particle Size Ratio $\sigma_2/\sigma_1 = 0.5$ but for equal effective masses ($m_1 = m_2$)	7.22

Tables

2.1	Analytical Instruments Associated with the Analytical Methods Development Subtask	2.1
2.2	CIA Standard and Synthetic Hanford Test Matrices	2.2
7.1	Major Components in Tank Wastes	7.3
7.2	Selected Tank Waste Compositions	7.4
7.3	Gibbsite Sedimentation Rates	7.14

1.0 Introduction

The Pretreatment Technology Development Project is one of seven Tank Waste Remediation System (TWRS) projects being conducted at Pacific Northwest Laboratory (PNL).^(a) A key objective of this project, which includes the Tank Waste Treatment Science Task, is to provide the technical basis and scientific understanding to support TWRS baseline decisions and actions, in particular, TPA Milestone M50-03, the 1998 sludge pretreatment decision regarding the level of pretreatment to be incorporated into the tank waste process flowsheets being developed by Westinghouse Hanford Company (WHC). This report details work performed by the Tank Waste Treatment Science Task during the first quarter of FY 1995 (October - December 1994) in support of the project objective. Specific activities are summarized below and further discussed in the main text.

Analytical Methods Development. To decrease analytical turnaround times; to increase sensitivity of the measurement; and/or to decrease waste volumes associated with obtaining analytical data for the project.

Sludge Dissolution Modeling. To provide the key thermodynamic data to be used in process flow-sheet development models and to provide a bounding case on dissolution reactions via direct experimental data on which tanks sludges will dissolve under specified processing conditions.

Sludge Characterization Studies. To identify the major solid phases in sludge; to determine how radionuclides are partitioned among the observed phases; to characterize the behavior of phases during processing; and to use the resulting database on sludge chemistry to help evaluate pretreatment technologies.

Sludge Component Speciation. To provide data on the chemical speciation of specific components in tank wastes that are important to developing pretreatment options. These data will allow predictions of how different tank wastes will respond to different pretreatment processes, as well as assist in the interpretation of existing pretreatment process chemistry data.

Pretreatment Chemistry Evaluation. To gather, evaluate, and integrate data on the characteristics of tank wastes that are relevant to the pretreatment end function.

Colloidal Studies for Solid-Liquid Separations. To determine how colloidal interactions in tank waste impact the major steps in tank waste processing, in particular, solid-liquid separations, as a function of waste processing conditions.

It is important to note that the scope of activities for the Tank Waste Treatment Science Task encompasses all aspects of tank waste processing. It is also important to recognize that there are complementary efforts going on at Hanford and at other U.S. Department of Energy sites as part of the Underground Storage Tank Integrated Demonstration (USTID) and Efficient Separations Processes

(a) Operated for the U.S. Department of Energy by Battelle Memorial Institute under Contract DE-AC06-76RLO 1830.

Integrated Program (ESPIP). To make the most efficient use of our resources, all possible effort is being made, and will continue to be made, to keep the lines of communication open among these activities to avoid duplication of effort and, most importantly, to create a cooperative, synergistic environment for performing the required technical work.

2.0 Analytical Methods Development

Brian M. Rapko

Activities for this subtask include purchasing and installing several analytical instruments. Table 2.1 summarizes the instruments to be installed and/or optimized during FY 1995. These instruments were selected to shorten some analytical turnaround times and/or increase the sensitivity of the measurement and/or decrease the waste volumes associated with obtaining analytical data. However, these new instruments, which in some cases introduce new analytical methods, will require some developmental work to be optimized for the complex and unique matrices associated with the TWRS sludge pretreatment project.

Work performed during the first quarter of FY 1995 resulted in the preparation and approval of a test plan for this subtask and the installation of two instruments: a particle size analysis system and a capillary ion analyzer (CIA). The particle size analyzer was designed by Particle Sizing Systems, Santa Barbara, California. The CIA was purchased from Waters/Millipore (Milford, Massachusetts).

2.1 Particle Size Analysis System

This system analyzes particles in two regimes. The first, which correlates the Brownian motion of the particles to the size, measures particles ranging from approximately 0.015 μm to 1 μm in size. In the second regime, the system measures the time it takes for a particle to pass a laser beam of known width in a flow-through cell and measures particles from approximately 0.5 μm to 400 μm in size. Both regimes utilize a common software package for data collection and processing. During the first quarter of FY 1995, the instrument was installed and size distributions of known standards (covering both regimes) were measured. Good agreement between the standards and the instrument measurements was observed.

Table 2.1. Analytical Instruments Associated with the Analytical Methods Development Subtask

<u>Instrument</u>	<u>Analytical function</u>	<u>Subtask purpose</u>
Capillary ion analyzer	Cation/anion analysis in Hanford tank pretreatment matrices	Installation assistance and method optimization
PERALS spectrometer	TRU identification and quantification	Installation and method optimization
Atomic absorption spectrometer	Cs analysis in dissolved Hanford tank pretreatment matrices	Installation and method optimization
Particle size analyzer	Determination of particle sizes	Installation assistance and method optimization

2.2 Capillary Ion Analyzer

This instrument is designed to analyze ions based on the method of capillary electrophoresis. In capillary electrophoresis, the different migration times of ions under an applied field are used to provide ion separation. Detection is generally accomplished by measuring absorbance changes at a specific wavelength. Filters and lamps for two wavelengths (254 nm and 185 nm) are currently available.

The method of detection at 254 nm is used for anion analysis in conjunction with a chromate-based electrolyte solution. Most simple inorganic anions do not absorb strongly at this wavelength. Consequently, at the point they pass through the detector, they displace the chromate ions in the electrolyte and decrease the solution's absorbance. This "indirect" method of detection has high sensitivity due to the strong absorbance of chromate at 254 nm. In addition, since no other ions absorb as strongly as chromate at this wavelength, the presence of any other anions will always cause a net absorbance decrease.

The other method of detection is to directly detect the absorbance of ions at 185 nm. Here, all of the simple inorganic anions of interest have an absorbance. However, the magnitude and direction of the change depends on the differences between the absorbance of the electrolyte and of the anion at this wavelength. Conceivably, for certain anion/electrolyte combinations, no absorbance change would result, and an analyte could pass through undetected. Therefore, the indirect method of detection is generally preferred for anions whenever possible.

After the CIA was installed, a standard solution was prepared to test it (Table 2.2). In addition, a series of test solutions were prepared that were designed to test "typical" solutions that might be encountered from testing of the enhanced sludge washing procedure (Lumetta and Rapko 1994) on Hanford tank sludges. These test solutions contained anion concentrations that were comparable to those measured for solutions derived from enhanced sludge washing of a composite sludge from Tank B-201, as determined by ion chromatography. The composition of the test solutions is also indicated in Table 2.2.

Table 2.2. CIA Standard and Synthetic Hanford Test Matrices

Label	Standard	A	B	C	D	E
F	1	7.5	7.5	210	210	7.5
Cl	2	21	21	41	41	21
Br	4	0.5	0.5	7	7	0.5
NO ₂	4	20	20	40	40	2
NO ₃	4	58	58	990	990	58
PO ₄	4	1	1	30	30	1
SO ₄	4	1	1	20	20	1
CO ₃	4	NA	NA	NA	NA	NA
OH	NA	NA	310	NA	310	NA

The standards were run using a set of initial conditions described in the instrument's operations manual and compared with the expected peak shapes and separation times. Excellent agreement was observed, indicating that the instrument was functioning. However, using these conditions with Test Solution A revealed separation problems. Resolution of sulfate, nitrite, and nitrate was poor, and resolution of fluoride and phosphate was marginal. A series of modifications were then examined with the Test Solutions B-E. These modifications included 1) decreasing the voltage to see if separation of the problem anions could be improved (at the cost of longer analysis times) and 2) using direct detection with a nitrate electrolyte to mask nitrate (which is often found in concentrations significantly higher than other anions of interest). The reasoning behind the second modification was that, if the loss of the intense nitrate signal by masking with the nitrate electrolyte allowed resolution of nitrite and sulfate, this information, together with measurement of the combined sulfate/nitrite/nitrate signal by the indirect method, might then allow the nitrate signal to be determined by difference.

Decreasing the voltage did not improve the resolution. On the contrary, analysis of the standard solution indicated that resolution performance decreased with decreasing voltage. Use of the indirect method also proved unsatisfactory. Not only did the resolution not improve but some anions appeared as positive peaks and others as negative peaks, which added greatly to the difficulty in interpreting the chromatogram. However, it was found that when the matrix nitrite concentration is small compared with nitrate and comparable to sulfate, sufficient resolution of the anions is obtained. Based on these results, subsequent analytical methods will focus on the use of either a combination nitrate/nitrite electrolyte or a nitrite-based electrolyte to mask nitrate/nitrite or nitrite, respectively. If successful, this should allow detection and quantification of the anions of most interest, namely, fluoride, chloride, sulfate, and phosphate.

2.3 Reference

Lumetta, G. J., and B. M. Rapko. 1994. *Washing and Alkaline Leaching of Hanford Tank Sludges: A Status Report*. PNL-10078, Pacific Northwest Laboratory, Richland, Washington.

3.0 Sludge Dissolution Modeling

Andrew R. Felmy

The keys to understanding the dissolution behavior of Hanford tank sludges involve identification of the important solid phases that are present in the sludges or that could form during pretreatment processing; identification of the range of pretreatment processing conditions, such as acid/base content, temperature, and electrolyte concentration over which these phases are likely to dissolve or be stable; identification, at least qualitatively, of the rates of the important dissolution reactions; and knowledge of the aqueous species/ion interactions that occur in the aqueous pretreatment solutions.

Thermodynamic modeling of the dissolution process provides a bounding case on the dissolution reactions and can provide direct information on which tank sludges should dissolve and under what conditions. Such information is essential in designing effective pretreatment strategies, and the data developed in this subtask will be of direct use to process flowsheet modeling efforts. In the first quarter of FY 1995, work was initiated in five areas:

1. Completing the model for the major electrolyte components, i.e., Na, NO_3 , NO_2 , SO_4 , CO_3 , F, PO_4 , OH, and $\text{Al}(\text{OH})_4$ in the Hanford tank wastes and developing the parameters for the Environmental Simulation Program (ESP) model.
2. Developing the necessary standard chemical potentials and ion-interaction parameters to include the alkaline earth cations: calcium, magnesium, and strontium. Including calcium and magnesium is important in order to model calcium and magnesium phosphates.
3. Developing the necessary data for important actinide elements, primarily plutonium and neptunium.
4. Initiating studies to include bismuth in the model, beginning with work on BiPO_4 .
5. Initiating work on necessary code modifications to model mineral dissolution rates and calculate the initial dissolution rate constants for selected solids for including in the ESP model.

The following text summarizes progress made in these areas during the first quarter of FY 1995. In addition, publications resulting from this task are listed.

3.1 Major Electrolyte Studies

Work focused on three major activities: 1) completing ongoing osmotic studies of Na_2CO_3 at 50°C and 100°C to complete the model for the major electrolyte components of the Hanford tank wastes; 2) implementing necessary computer code modifications to calculate the parameters for the ESP model; and 3) performing model validation calculations on NaNO_3 and NaNO_2 solubility in simulated nuclear wastes.

3.1.1 Complete Ongoing Osmotic Studies

The necessary isopiestic data to get osmotic coefficients for Na_2CO_3 at 50°C have been obtained. Experiments have also been initiated to obtain isopiestic data for Na_2CO_3 at 100°C . These data are necessary to complete the model of the major binary electrolytes extending from 25°C to 100°C .

3.1.2 Implement Computer Code Modifications

These modifications are being implemented to utilize the existing parameter calculation code NONLIN to calculate the parameters for the ESP model. These code modifications will be tested by comparison with the existing ESP code. Modifying the existing code allows existing data files on solubility and osmotic data to be used to calculate the ESP parameters. Existing ESP fitting routines are very cumbersome when ion association species are included in the treatment.

3.1.3 Perform Model Validation Calculations

The existing model for the major electrolyte components of tank wastes was tested by comparing predicted solubilities of NaNO_3 and NaNO_2 in simulated nuclear waste with direct experimental observations. These results, depicted in Figures 3.1 and 3.2, show that the model gives very reliable predictions for the solubility of NaNO_3 at 60°C and 80°C . The model also works well to predict NaNO_2 solubility at 60°C (Figure 3.3). However, the model slightly underpredicts the solubility of NaNO_2 at 80°C (Figure 3.4). These results are very encouraging and demonstrate the usefulness of the model developed from simple systems to predict concentrations in simulated complex tank solutions (i.e., mixtures of sodium nitrates, nitrites, and hydroxides).

3.2 Alkaline Earth Cation Inclusion

Inclusion of magnesium, calcium, and strontium into the thermodynamic solubility model for Hanford tank sludge requires evaluation of the interactions between these species and other important solution components such as NO_3^- , NO_2^- , SO_4^{2-} , CO_3^{2-} , F^- , PO_4^{3-} , OH^- , and $\text{Al}(\text{OH})_4^-$. Work to date has focused on three activities: 1) locate and organize thermochemical data available in the literature from which model parameters may be evaluated; 2) identify those subsystems/interactions for which data are not available and design suitable experiments for their evaluation; and 3) procure necessary chemicals to conduct the experiments.

3.2.1 Locate/Organize Thermochemical Data

Potentially useful experimental data were located from a variety of literature sources. These data include isopiestic and solubility measurements on a number of subsystems of interest in the present investigation. Available solubility data extend to 100°C in some cases; however, osmotic data above room temperature are notably absent.

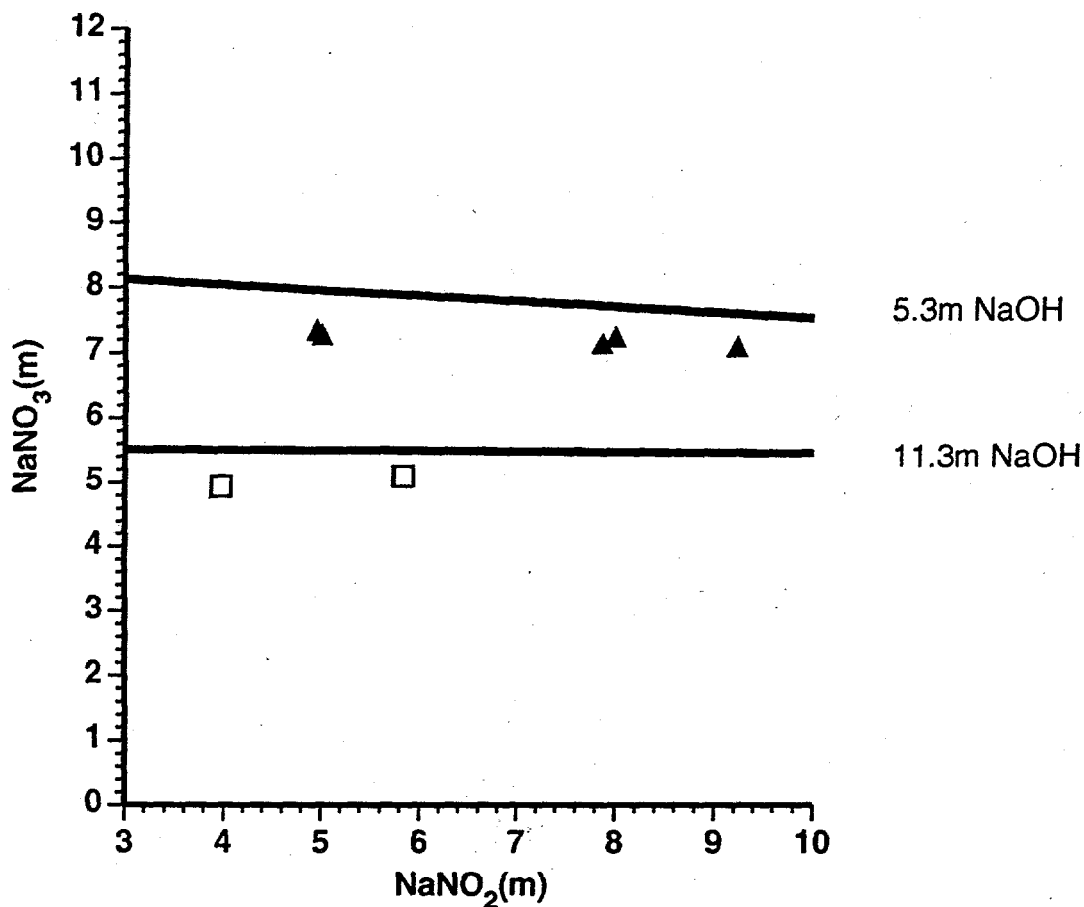


Figure 3.1. Experimental and Calculated Solubilities of NaNO₃ at 60°C. Experimental data of Reynolds and Herting (1984).

3.2.2 Identify Subsystems/Interactions for which Data Are Not Available

Additional data, beyond those found in the literature and required to complete the database for evaluation of parameters in the thermochemical model, have been identified, and appropriate experiments have been planned for collecting these data. Specifically, isopiestic experiments at $T > 25^{\circ}\text{C}$ are planned for the highly soluble nitrates and nitrites of the cations listed above, while additional solubility experiments will be performed as required in the various binary and common-ion ternary subsystems.

3.2.3 Procure Chemicals

Chemical reagents necessary for the above experiments have been procured from commercial vendors where possible, and procedures for laboratory synthesis of others are currently being developed (some of the nitrites).

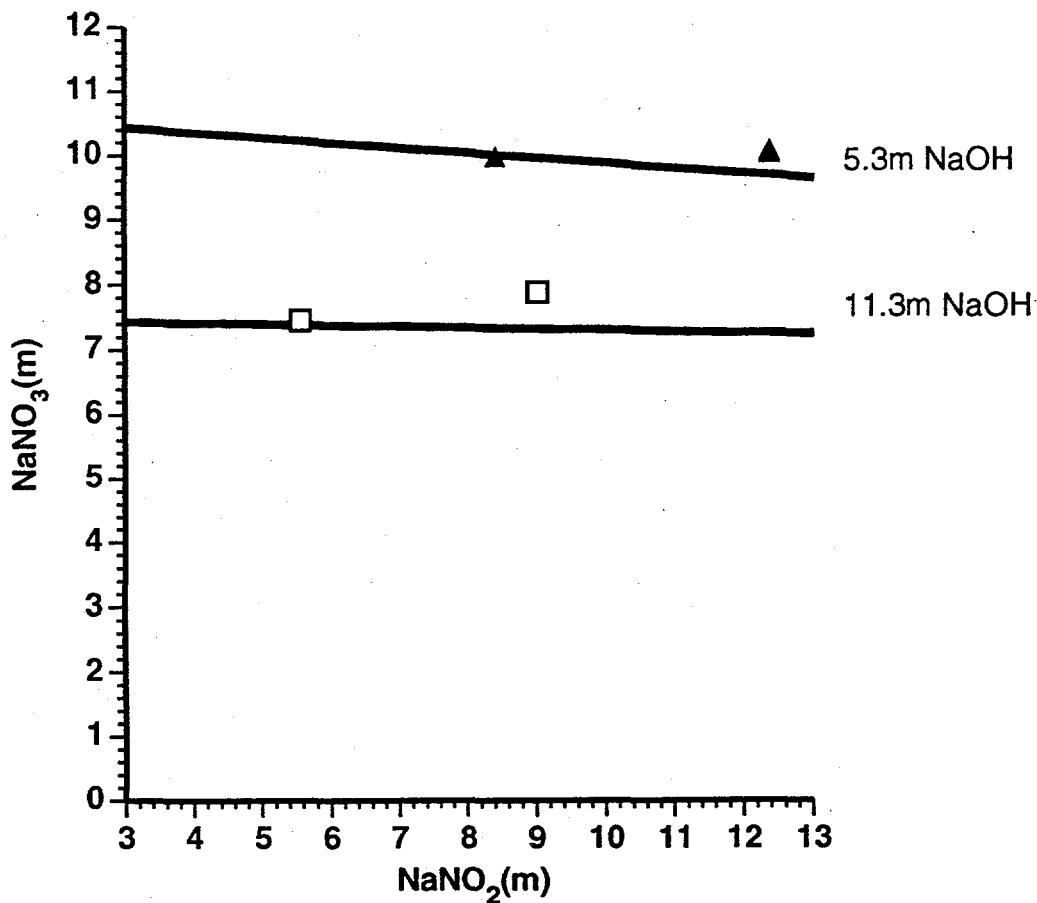


Figure 3.2. Experimental and Calculated Solubilities of NaNO_3 at 80°C .
Experimental data of Reynolds and Herting (1984).

3.3 Actinide Studies

Meetings were held with C. H. Delegard at WHC to discuss some of his previous studies on PuO_2 solubility in concentrated electrolytes such as NaOH , NaNO_3 , NaNO_2 , and NaAl(OH)_4 and to develop a plan for analyzing these data to obtain the necessary model parameters. A study plan was outlined to obtain the necessary information on the aqueous species present in these solutions. This information is necessary to develop an accurate chemical model for Pu dissolution in the waste tanks.

Parallel solubility studies using Np(V) as a model for Pu(V) have been planned. Spectroscopy (ultraviolet, visible, near infrared) is one of the techniques to be used for speciation. The start date for the experimental work is contingent on the instrument servicing arrangements and radiation zoning.

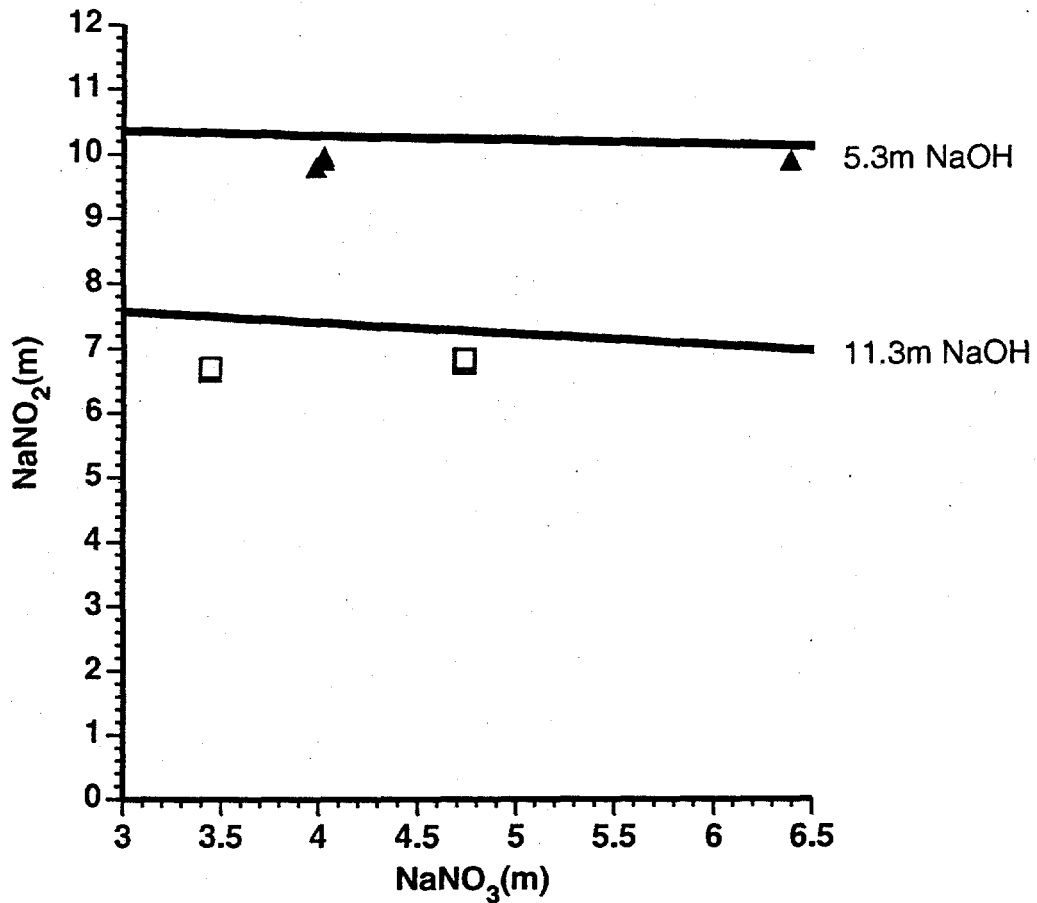


Figure 3.3. Experimental and Calculated Solubilities of NaNO₂ at 60°C. Experimental data of Reynolds and Herting (1984).

3.4 Bismuth Studies

Staff have been assigned to this task, and an initial literature search for BiPO₄ solubility data has been conducted. Preliminary plans for BiPO₄ experiments are being formulated.

3.5 Kinetic Modeling

Plans were outlined to make necessary code modifications for calculating and using data on mineral dissolution rates. These rate data also will be put in a form for use in the ESP model.

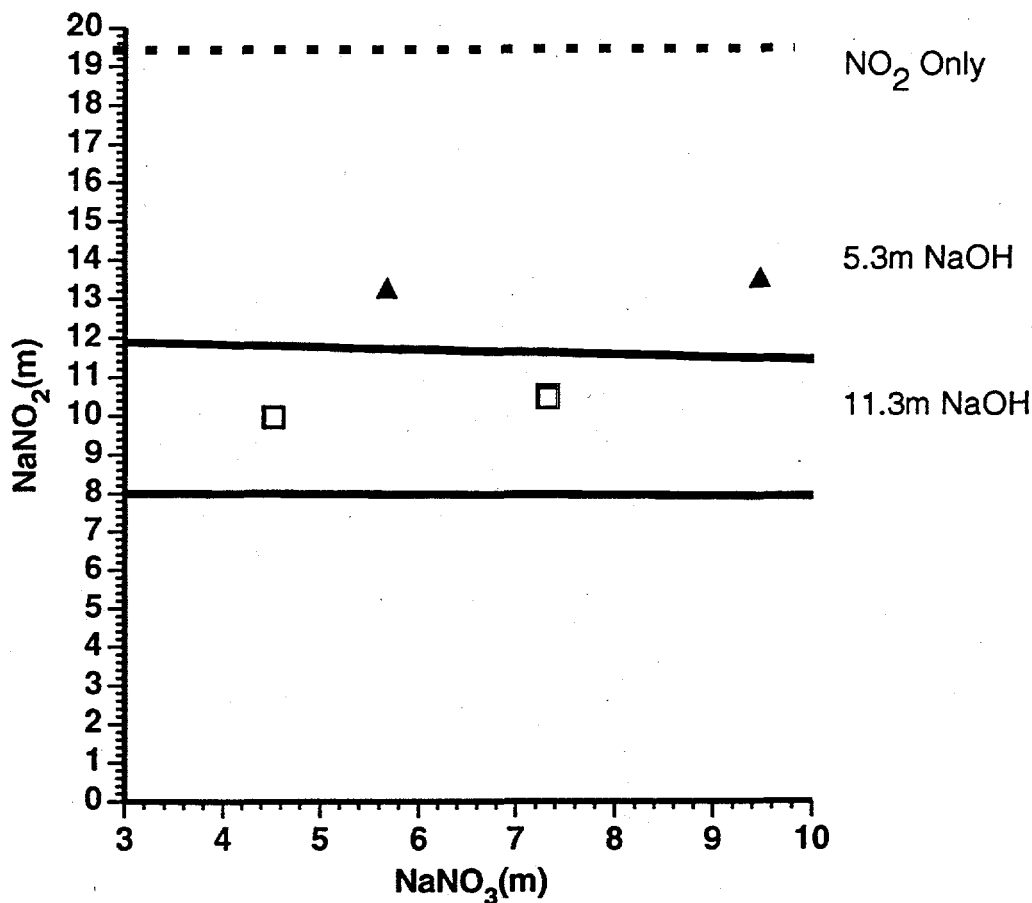


Figure 3.4. Experimental and Calculated Solubilities of NaNO₂ at 80°C. Experimental data of Reynolds and Herting (1984).

3.6 Publications

Three papers were submitted for publication in the ACS Symposium Series on Scientific Issues Related to Safety and Treatment of Hanford Wastes:

Felmy, A. R., J. R. Rustad, M. J. Mason, and R. de la Bretonne. *A Chemical Model for the Major Electrolyte Components of the Hanford Waste Tanks: The Binary Electrolytes in the System: Na-NO₃-NO₂-SO₄-CO₃-F-PO₄-OH-Al(OH)₃-H₂O.*

Felmy, A. R., D. Rai, and R. W. Fulton. *The Solubility of Cr(OH)₃(am) in Concentrated NaOH and NaOH-NaNO₃ Solutions.*

Felmy, A. R., C. C. Schroeder, and M. J. Mason. *A Solubility Model for Amorphous Silica in Concentrated Electrolytes.*

3.7 Reference

Herting, D. L., and D. A. Reynolds. 1984. *Solubilities of Sodium Nitrate, Sodium Nitrite, and Sodium Aluminate in Simulated Nuclear Waste*. RHO-RE-ST-14P, Rockwell Hanford Operations, Richland, Washington.

4.0 Sludge Characterization Studies

Jun Liu and Larry E. Thomas

The objectives of this subtask are to identify the major solid phases present in sludge; determine how radionuclides are partitioned among the observed phases; characterize the ion exchange, colloidal chemistry, and dissolution behavior of phases during sludge processing; and use the resulting database on sludge chemistry to help evaluate existing sludge pretreatment technologies and develop new sludge pretreatment schemes. Work within this subtask is divided into three activities: 1) transmission electron microscopy (TEM) analysis of actual sludges; 2) TEM analysis of simulated sludges; and 3) supplemental analysis of sludges by x-ray diffraction (XRD) and nuclear magnetic resonance (NMR). XRD provides additional information on the crystalline structure of compounds, and NMR provides information about the chemistry and chemical reactions in simulants.

Two samples from Tank T-111 (one untreated core sample and the other treated by enhanced washing) were received in December, and TEM characterization of these two samples has begun.

5.0 Sludge Component Speciation

David L. Blanchard, Steven D. Conradson (LANL), Richard L. Gordon,
Nancy J. Hess, J. Craig Hutton, Marc M. Lamoureux, and David L. Styris

The chemical speciation of sludge components is perhaps the single most important factor in determining how they will respond to any chemical processing. For example, in the current baseline strategy, a large fraction of the phosphorus and chromium must be removed from the sludge in order to minimize the volume of high-level waste that is produced. The key to designing an effective pretreatment strategy is knowing whether the phosphorous is present as BiPO_4 , $\text{Ca}_3(\text{PO}_4)_2$, or some other low soluble form, such as calcium hydroxy-apatite $[\text{Ca}_5(\text{OH})(\text{PO}_4)_3]$ or apatite $[\text{Ca}_5\text{F}(\text{PO}_4)_3]$. How much AlPO_4 , $\text{Mn}_3(\text{PO}_4)_2$, $\text{Sr}_3(\text{PO}_4)_2$, and $\text{Ba}_3(\text{PO}_4)_2$ is present? Are there any phosphite species? Is chromium in the sludge found in pure phases, such as Cr_2O_3 , CrO_3 , $\text{Na}_2\text{Cr}_2\text{O}_7$, or Na_2CrO_4 , or in minerals such as FeCr_2O_4 ? Because these solids have different solubilities that vary extensively with pH and the concentration of other ions, the extent of phosphorus and chromium removal will be determined by these details. In addition, chemical speciation data will allow us to understand future technology development, should it be needed.

Chemical speciation is defined in this context as identification of the chemical compounds and phases and the *physical location* (e.g., co-precipitation vs. precipitation in separate phases, or at the surface of another phase, etc.) of sludge constituents. This information is required because elemental information is not sufficient for predicting how a complex mixture will respond to a given treatment. The purpose of this subtask is to provide data on the chemical speciation of specific components of tank wastes that are important to developing the pretreatment baseline. These data will allow predictions of how different tank wastes will respond to pretreatment processes, as well as assist in the interpretation of existing pretreatment process chemistry data.

In FY 1994, this subtask performed a survey of existing analytical techniques for chemical speciation. As a result of this study, x-ray absorption spectroscopy (XAS) and laser ablation/mass spectroscopy (LA/MS) were chosen as the most appropriate techniques for providing speciation information. In addition to the ability to provide this information, these techniques require minimal sample preparation and disruption during measurement. These techniques also are complementary. XAS can readily provide information on low concentration elements (down to 10 ppm) that may not be present in pure phases. Such inclusions are more difficult to identify with LA/MS techniques. In turn, LA/MS is very effective at identifying organic species and compounds of low atomic weight elements, which are difficult to identify with XAS.

The following sections detail first quarter progress in the use of XAS and LA/MS for identifying species in tank sludges to support TWRS Pretreatment Technology Development.

5.1 X-ray Absorption Spectroscopy

5.1.1 Presentations

Several presentations were given on the preliminary study of tank sludges. N. J. Hess gave a talk October 18, 1994, entitled "Application of XAS to Environmental Remediation and Restoration" at the

Stanford Synchrotron Radiation Laboratory (SSRL) Users Meeting, Stanford Linear Accelerator Center (SLAC). Some of the results from the preliminary study of tank sludges with XAS (in FY 1994) were presented. On October 19, S. D. Conradson presented a talk entitled "Application of XAS to Actinide Problems" at the Workshop on Analytical Applications of Synchrotron Radiation: Environmental and Materials Science. This talk also contained results from the preliminary XAS study of tank sludge. Later, the floor was opened to questions from the participants about the new Environmental Beamline. (Questions were answered by a panel that included R. L. Gordon from PNL). This beamline has been funded for construction at SSRL beginning this fall. Although facilities such as hoods or glove boxes will not be available to work with open radioactive samples, experiments with contained radioactive samples on this beamline are encouraged. This will be a very valuable facility for studies of radioactive materials associated with the Hanford cleanup, including tank waste.

A seminar entitled "Speciation of Sr and Ni in Tanks C-112 and C-109 Sludges" was presented by D. L. Blanchard, J. C. Hutton, and R. L. Gordon at PNL on October 13. Data from the FY 1994 preliminary study of XAS of tank sludges were presented. G. T. MacLean, who leads the Sludge Dissolution Modeling task at WHC, indicated that PNL results from XAS speciation analysis of wastes from Tanks C-109 and C-112 (in FY 1994) helped to gain a better understanding of the solid phases present in the waste, which is important for predicting the results of leaching and washing of the sludges.

5.1.2 XAS Testing

Eight sample holders and two sample assemblies for XAS experiments on radioactive samples were fabricated at Los Alamos National Laboratory (LANL) and shipped to PNL. Each sample holder will hold 0.4 ml of sample. In FY 1994, there were some problems with corrosion of the holders after loading because the alkaline samples and the aluminum holders were incompatible. The new holders have been fabricated from a commercially available corrosion-resistant alloy, which should prevent such problems. The sample assemblies hold four sample holders, and provide two more containment barriers and shielding. These will be used for the run at SSRL expected to be scheduled in March.

Sample analysis has been coordinated with the TWRS Sludge Treatment Technology Task. Experiments will include analysis of elements that are left undissolved after sludge washing and leaching in an attempt to identify species that resist pretreatment efforts and to determine whether any species have metathesized during the process.

5.2 Laser Ablation/Mass Spectrometry

This technique appears to require some development in order to provide speciation information. Therefore, simulants will be run initially to determine the utility of this technique for speciation information. Experiments on simulants will focus on aluminum, phosphorus, strontium, chromium, and others.

6.0 Pretreatment Chemistry Evaluation

*Penny Colton, Gregory S. Anderson, John L. Cox,
Everett A. Jenne, Julian G. Hill, and Antonio J. Villegas*

The objective of this subtask is to gather, evaluate, and integrate data on the characteristics of tank wastes that are relevant to the pretreatment end function. Activities within this subtask include:

Process Chemistry Evaluation. Chemical analyses data and chemical flowsheet compositions are being used to define waste stream compositions in terms of chemical species that are present in the tanks. Also, a literature search on the dissolution and metathesis behaviors of important species identified in sludges will be performed. The results from these activities will provide insight into the partitioning behavior of different waste streams during pretreatment processing, as well as insight into the chemical composition of the waste streams that are sent to high-level waste vitrification.

Data Evaluation Using the Sort on Radioactive Waste Type (SORWT) Model. This activity is focused on 1) systematically determining how physical properties vary from tank to tank and across SORWT groups and 2) using an electronic data set of historical sample analyses to generate tank-by-tank estimates of waste characteristics. These tank-by-tank estimated compositions based on analysis will be compared with chemical inventories predicted by LANL.

During the first quarter FY 1995, efforts in these activities centered on data gathering. The work conducted is discussed in the following sections.

6.1 Process Chemistry Evaluation

Early efforts in this activity focused on defining the aluminum- and silicon-containing species in the waste inventory. Work is currently under way to define the chemical species in the LANL "defined waste streams" (Agnew 1994). The results from this effort will be used to establish separation factors on a tank-by-tank basis.

6.1.1 Silicon

EIS source document (Stordeur 1986):	446 t Si
Estimated inventory document (Allen 1976):	417 t Si
Hanford defined waste compositions (Agnew 1994):	540 t Si

Single-Shell Tank (SST) Inventory

The estimated inventory (Allen 1976) included chemicals used in processing through 1975 and did not include chemicals used in the PUREX process after that time. The silicon-containing species were estimated with the assumption the silicon inventory that originated in processing streams was closer to 540 t Si.

Cancrinite ($\text{Na}_8\text{Al}_6\text{Si}_6\text{O}_{24}\cdot 2\text{NO}_3$). During experiments at WHC, cancrinite was synthesized in highly alkaline solutions that contained sodium, aluminum, silicon, and nitrate ions. These conditions

were present in aluminum cladding waste streams. Silicon also was present in PUREX waste streams that contained virtually no aluminum. If these silicon-containing PUREX wastes were mixed with other wastes that contained aluminum, cancrinite could potentially form if conditions were suitable. Assuming that aluminum cladding waste produced cancrinite (137 t Si) and that additional PUREX streams may have contributed to cancrinite formation: **368 t Si**.

Sodium Silicate. The second decontamination cycle BiPO_4 (2C) waste streams contained silicon and very little aluminum. The aluminum silicate species that was identified in this type of waste by x-ray diffractometry was not cancrinite. One possible explanation is that this waste stream was originally an acid stream that was neutralized to a pH around 10; thus, the highly alkaline conditions did not exist for cancrinite to form. Based on wash/leach data for Tank B-110 that contains 2C waste, about 10% of the sodium silicate might be removed in the wash, and potentially another 60% might be removed with alkaline leaching. The 2C wastes do not appear to have been mixed with other aluminum-containing wastes. Assuming silicon from 2C is sodium silicate (less 18 t that may have been transferred in supernatant to double-shell tanks (DSTs): **87 t Si**.

In addition, silicon was added to the tanks in the form of Portland cement (1 tank) and diatomaceous earth (6 tanks), and blowsand is believed to have entered the tanks during tank farm operations.

Quartz (SiO_2). Quartz is a major constituent in Hanford soils: **18 - 72 t Si**.

Diatomaceous earth (354 t, ~30% Si): **106 t Si**.

Portland cement (57 t, ~10% Si): **5.7 t Si**.

An additional 3 t of silicon may have originated in the PUREX process in the form of an antifoam agent during the sugar denitration step.

Double-shell Tank Inventory

Estimated mass: **5.6 t soluble Si, 79 t insoluble Si**.

These inventories should be consistent with inventories reported in the EIS source document.

6.1.2 Aluminum

EIS source document (Stordeur 1986):	2660 t Al
Estimated inventory document (Allen 1976):	10800 t Al
Hanford defined waste compositions (Agnew 1994):	6950 t Al
George Borsheim (WHC) calculations:	6200 t Al

Single-Shell Tank Inventory

The EIS aluminum inventory appears low; using the EIS value, the aluminum in 27 SSTs that have been characterized accounts for 31% of the SST aluminum inventory. The bulk aluminum-containing species in the tank waste were estimated assuming the aluminum inventory was closer to 6950 t Al.

Cancrinite ($Na_8Al_6Si_6O_{24} \cdot 2NO_3$). Refer to discussion on cancrinite in silicon section above:
355 t Al.

Sodium Aluminate ($NaAlO_2$). Based on data for 8 salt cake-type wastes in Schulz (1980) $\leq 1\%$ of salt cake is aluminum. Assuming 1% of the 135,000 t of salt cake and 12,000 t of interstitial liquid (Stordeur 1986) is salt cake: 1470 t Al.

Gibbsite/Boehmite [$Al(OH)_3/AlOOH$]. The remainder of the aluminum is assumed to be either gibbsite or boehmite, two hydrated aluminum oxide species, i.e., aluminum hydroxides, that have been identified in sludges using x-ray diffractometry (In waste from Tank U-110, approximately 75% to 85% of the aluminum was in the form of gibbsite.): 3970 t Al.

Albite ($NaAlSi_3O_8$). Albite is a major constituent in Hanford soils. Soil or blowsand is believed to have entered the tanks during tank farm operations: 3 - 12 t Al.

Double-shell Tank Inventory

Estimated mass: 1090 t soluble Al, 64 t insoluble Al.

These inventories should be consistent with inventories reported in the EIS source document.

6.2 Data Evaluation Using the Sort on Radioactive Waste Type (SORWT) Model

The SORWT model (Hill et al. 1995) has been used successfully to categorize Hanford SSTs into groups of tanks that are expected to exhibit similar chemical and physical characteristics based on their major waste types and processing histories. This methodology is being used to look at the variability in physical properties across individual tanks and SORWT groups, as well as to evaluate a historical sample analysis data set to provide a tank-by-tank estimate of analyte concentrations.

6.2.1 Evaluation of Physical Properties

The data structure for the statistical analysis of physical and rheological tank waste properties is fully developed. Modifications to the data structure may occur as data continue to be entered. The following parameters are currently being considered for the statistical analysis:

- Shear Strength
- Yield Point
- Viscosity
- Critical Reynold's Number for Turbulent Flow
- Weight Percent Water

- Weight Percent Undissolved Solids
- Volume Percent Settled Solids
- Density
- Particle Size.

S-Plus (StatSci, Seattle, Washington) will be the primary statistical software package used in the analysis. An analysis of variance will be the primary test for measuring the variability of physical and rheological properties across tanks and SORWT groups. The results of the analysis may lead to improvements in the SORWT model and a better understanding of characterization data needs.

6.2.2 Evaluation of Historical Data Set

An electronic copy of a tank waste database (commonly referred to as the "Braun data set" or "Braun database") has been obtained from D. J. Braun and T. M. Brown of WHC. This database contains over 16,000 records with information about samples taken from the tanks, i.e., analyte concentrations, date the sample was taken, the reference document that cites the sample results, and additional physical property information about the samples. Data not relevant to this project have been deleted to reduce the size of the database. Also during this quarter, a meeting was held to determine what statistical techniques should be considered for evaluating the database in conjunction with the SORWT model.

6.3 References

- Agnew, S. F. 1994. *Hanford Defined Wastes: Chemical and Radionuclide Compositions*. LA-UR-94-2657, Los Alamos National Laboratory, Los Alamos, New Mexico.
- Allen, G. K. 1976. *Estimated Inventory of Chemicals Added to Underground Waste Tanks, 1944 Through 1975*. ARH-CD-610-B, Atlantic Richfield Hanford Company, Richland, Washington.
- Hill, J. G., G. S. Anderson, and B. C. Simpson. 1995. *The Sort on Radioactive Waste Type Model: A Method to Sort Single-Shell Tanks into Characteristic Groups*. PNL-9814 Rev. 2, Pacific Northwest Laboratory, Richland, Washington.
- Schulz, W. W. 1980. *Removal of Radionuclides from Hanford Defense Waste Solutions*. RHO-SA-51, Rockwell Hanford Operations, Richland, Washington.
- Stordeur, R. T., et al. 1986. *Hanford Defense Waste Disposal Alternatives Engineering Support Data for the HDW-EIS*. RHO-RE-ST-30P, Rockwell Hanford Operations, Richland, Washington.

7.0 Colloidal Studies for Solid-Liquid Separation

Bruce C. Bunker, Gordon L. Graff, Peter A. Smith, Yong Wang,
Paul J. Bruinsma, David R. Rector, Jun Liu, and Lin Song

Tank waste sludges contain fine particles of insoluble oxides, hydroxides, and salts. During many critical phases of tank waste processing, these insoluble particles will be mixed with aqueous solutions, and colloidal suspensions will form. The Colloidal Studies subtask is aimed at understanding and modeling the behavior of such colloidal suspensions and determining how colloidal interactions impact major steps in tank waste processing.

Figure 7.1 is a generic representation of the current baseline flowsheet for tank waste processing. The first class of processing steps involves processes such as sluicing to produce an aqueous suspension of sludge particles that can be removed from individual tanks and pumped to centralized processing facilities. For retrieval and transport, the desire in the baseline process is to produce sludge slurries that have the maximum solids loadings (to minimize waste volumes) and that still have sufficiently low viscosities to allow pumping for distances up to 6 miles.

The second class of processing steps consists of in-tank processing steps that include storage, leaching, and washing. Here, settle-decant operations are envisioned in which insoluble sludge components sink to the bottom of the tank under the force of gravity to provide solid-liquid separations. The resulting supernatant liquids, containing soluble salts, would represent the primary low-level waste (LLW) stream, while the insoluble sludge remaining behind would represent the high-level waste (HLW) stream. To have efficient settle-decant processing, the colloidal sludge suspensions must exhibit rapid sedimentation rates (> 3 cm/hr), and must form compact sediment beds that contain the minimum volume of interstitial liquids.

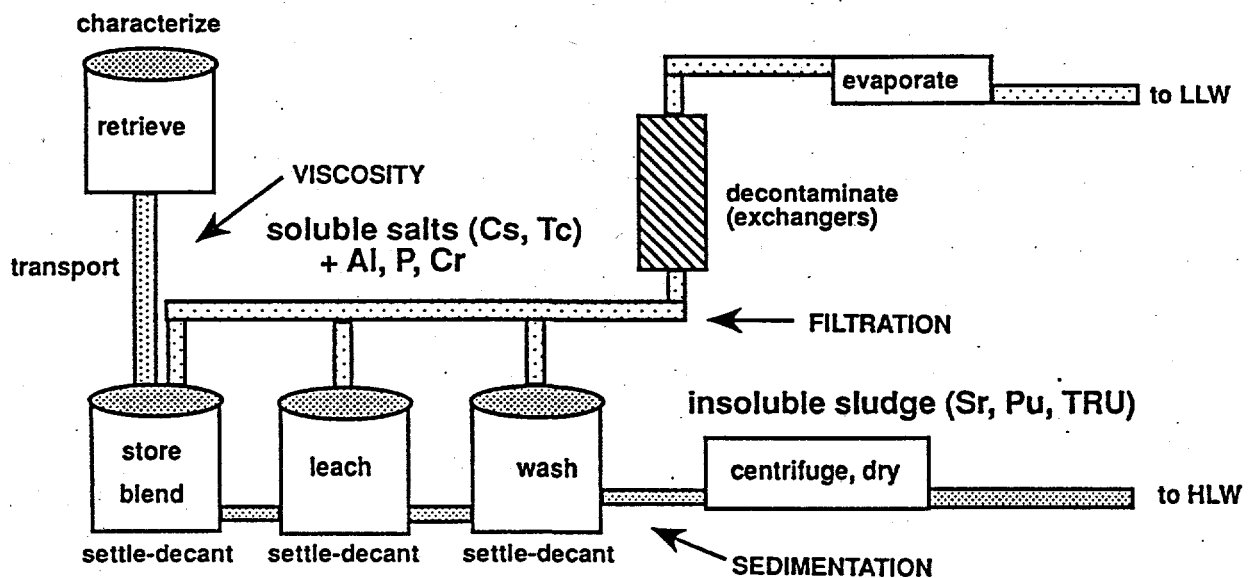


Figure 7.1. Major Steps in Tank Waste Processing

It is inevitable that the supernatant liquids sent to the LLW stream will contain a certain fraction of suspended particles that are not removed via settle-decant operations. A third class of processing is required to prevent having these suspended particles either contaminate the LLW stream or foul critical components such as ion exchangers used to remove soluble radioactive species like cesium. The baseline process for removal of the fine particulates in the supernatant liquids is filtration. Colloidal interactions are important in determining what particles remain suspended, and how easy or difficult it is to remove such particles via filtration.

The Colloidal Studies subtask consists of three major activities: 1) experimental studies aimed at characterizing the interactions between model colloids and the impact of those interactions on slurry properties such as viscosities, sedimentation rates, and filtration behavior; 2) theoretical studies aimed at developing mathematical models to describe, explain, and predict colloidal behavior; and 3) preparation of a facility to be designated as a Hot Colloids Laboratory in which predictions based on "cold" experimental studies on simulants and the theoretical models can be tested on real sludge samples. Work performed during the first quarter of FY 1995 in each of the above activities is summarized below and described in more detail in the following sections.

Experimental Studies. Colloidal suspensions of boehmite (AlOOH) and gibbsite [$\text{Al}(\text{OH})_3$] have been prepared and characterized in terms of primary particle size and shape, surface charge, and degree of agglomeration. Property measurements have been performed to determine how particle morphology, solids loadings, pH, and ionic strength influence slurry properties that include viscosity, sedimentation kinetics, and filtration.

Modeling Studies. Computer programs have been developed to model the rheological and sedimentation properties of colloidal suspensions. Models include Stokesian Dynamics methods for simulating the motions of solids particles in fluid suspensions and Monte Carlo methods for determining density profiles on concentrated colloidal suspensions in sedimentation equilibrium. Work has also been initiated to model transient sedimentation.

Hot Colloids Laboratory. Space is being identified for location of the laboratory. Existing equipment has been identified. Purchase orders for new capital items have been initiated.

7.1 Experimental Studies

7.1.1 General Particle Characterization

The Colloidal Studies subtask is investigating the properties of colloidal slurries that are representative of materials found in actual sludge. Model colloids have been selected on the basis of composition as well as particle size and shape. Elemental analyses of tank sludges indicate that the major insoluble components expected to be present (Table 7.1) are oxides and hydroxides of aluminum, iron, zirconium, and chromium, aluminosilicate minerals, and insoluble salts such as calcium phosphates. All of the above components are to be studied within this subtask both as individual components and

Table 7.1. Major Components in Tank Wastes

Element	Mass (tons)	Moles	Impact (comments)
Na	68,270	2.7×10^9	mainly soluble salts
Al ^(a)	4,840	1.6×10^8	key colloid, soluble species, cements, gels
P ^(a)	1,855	5.4×10^7	major glass problem, Sr location
Zr ^(a)	1,100	1.1×10^7	major insoluble colloid
Fe ^(a)	819	1.3×10^7	major insoluble colloid
Si ^(a)	506	1.6×10^7	not free, reacts to form gels, cements, clays
Cr	165	2.8×10^6	major glass problem

(a) Target species in colloid studies.

in mixed particle suspensions (with the possible exception of chromium). Insoluble particles are to be suspended in a range of different solutions. However, the emphasis will be on the high pH (pH 11-14) and high salt content (0.01 to 5 M NaNO₃) regime thought to represent the most probable range of processing environments.

Particle images obtained via transmission electron microscopy (TEM) provide information concerning the size and shape of particles having different compositions. The TEM images reveal that, while a broad range of particle sizes is present, over 50 vol% of the insoluble material in tank sludge is present as crystallites that are smaller than 1 μm in diameter. However, given the wide range of different sludge types present in the 177 Hanford tanks (e.g., Table 7.2), it is unlikely that a generic tank simulant having the composition shown in Table 7.1 will be capable of representing the range of behaviors expected for the wide range of particle mixtures represented in the tank farm. Therefore, work in this subtask is aimed at identifying how interactions between the colloids will vary with the compositions and mixtures of different particle types and solutions.

The most important chemical constituent in sludge from a processing standpoint is probably aluminum because it is present in large quantities. Although it is relatively soluble in high pH solutions representative of tank wastes, it is present in high enough concentrations that it can exist predominantly in the form of insoluble colloidal particles, as soluble species, or as mixtures of both, depending on total aluminum present and on solution parameters such as pH and temperature. Even for a single tank solution, changes in processing conditions can lead to either dissolution or reprecipitation of the aluminum-containing particles. TEM analyses suggest that aluminum is present in three major forms: as extremely fine particles (< 10 nm crystallites) of boehmite (AlOOH), as 1- to 40-μm particles of gibbsite (Al(OH)₃), and as aluminosilicate clay-like minerals that are submicron in size. Due to reasons of both prevalence and complexity, aluminum-containing solutions were selected as the first colloidal system for study.

Table 7.2. Selected Tank Waste Compositions

Element	102-SY (PFP)	105-AW (NCRW)	102-AZ (CC)	C-112 (TBPf/1C)	B-110 (2C)	C-103 (PUREX)
Na	2.8	4.8	9.2	4.8	--	1.9
Al	3.5	0.22	0.13	0.20	0.03	0.61
Fe	0.93	0.12	0.10	0.37	0.48	2.1
Zr	0.009	3.15	0.001	--	--	0.2
Si	0.19	0.36	0.002	0.41	0.44	2.7
Ca	0.31	0.03	0.02	0.32	0.02	0.29
B	0.05	0.12	0.002	0.09	--	--
U	0.014	0.12	0.003	0.003	--	0.01
Cr	0.65	0.03	0.004	0.004	0.02	0.001
Mn	0.35	0.03	0.02	0.02	--	--
Mg	0.16	0.014	0.003	0.003	0.006	0.05
Bi	--	--	--	--	0.11	0.004
NO _{3,2}	0.44	1.0	--	--	3.3	0.03
SO ₄	0.19	0.03	0.2	--	0.14	--
PO ₄	0.70	--	0.2	0.02	0.71	0.14
F	0.14	0.57	0.1	--	0.11	--

PFP: Plutonium Finishing Plant.

NCRW: Neutralized Cladding Removal Waste.

CC: Complexant Concentrate.

TBPf/1C: Tributyl Phosphate (ferrocyanide scavenged)/1st Decontamination Cycle BiPO₄.

2C: 2nd Decontamination Cycle BiPO₄.

PUREX: PUREX Waste.

Initial studies of colloidal interactions reported here are on suspensions of commercially available monodispersed gibbsite and boehmite suspensions. TEM images of the boehmite show that the primary particles in the commercial powder are 50-nm x 5-nm plates that are somewhat larger than the 10-nm crystallites seen in sludge samples to date. The commercial gibbsite has been obtained for three particle sizes (0.25, 1, and 10 μm) spanning sizes seen in real sludge samples. However, the commercial

materials are equiaxed blocky particles, while the material in tanks form needles with an aspect ratio of around 10. For initial studies, sodium nitrate solutions (0.01 M) containing 3, 6, and 10 vol% of either boehmite or gibbsite have been prepared, using nitric acid or sodium hydroxide to adjust the pH to 3, 7, 10, 12, and 14.

The final parameter required for initial characterization of colloidal particle slurries involves determining the extent to which particles interact with each other to form agglomerates. Agglomeration is sensitive to many solution parameters including pH, salt content, and the presence of organics. While the role of organics is a major part of this subtask, work reported in this quarter deals with interactions controlled by pH and ionic strength effects only.

In simple electrolyte solutions, two forces dominate the degree of agglomeration. The minimum interaction potential between two particles involves short-range van der Waals attractions (Figure 7.2). Such attractions will cause particles to stick to each other when they come within a few nanometers of each other. Opposing the van der Waals attractions are electrostatic repulsions associated with fixed charges on particle surfaces. For oxides, the fixed surface charges are associated with protonation and deprotonation of oxygen sites in the surface, which in turn are controlled by the solution pH. If an excess of protons is present, the surface is positively charged, while if a surface excess of anionic hydroxide groups is present, the surface is negatively charged. In either case, charge-compensating ionic clouds surrounding the particles can extend for distances of microns when the particles are in

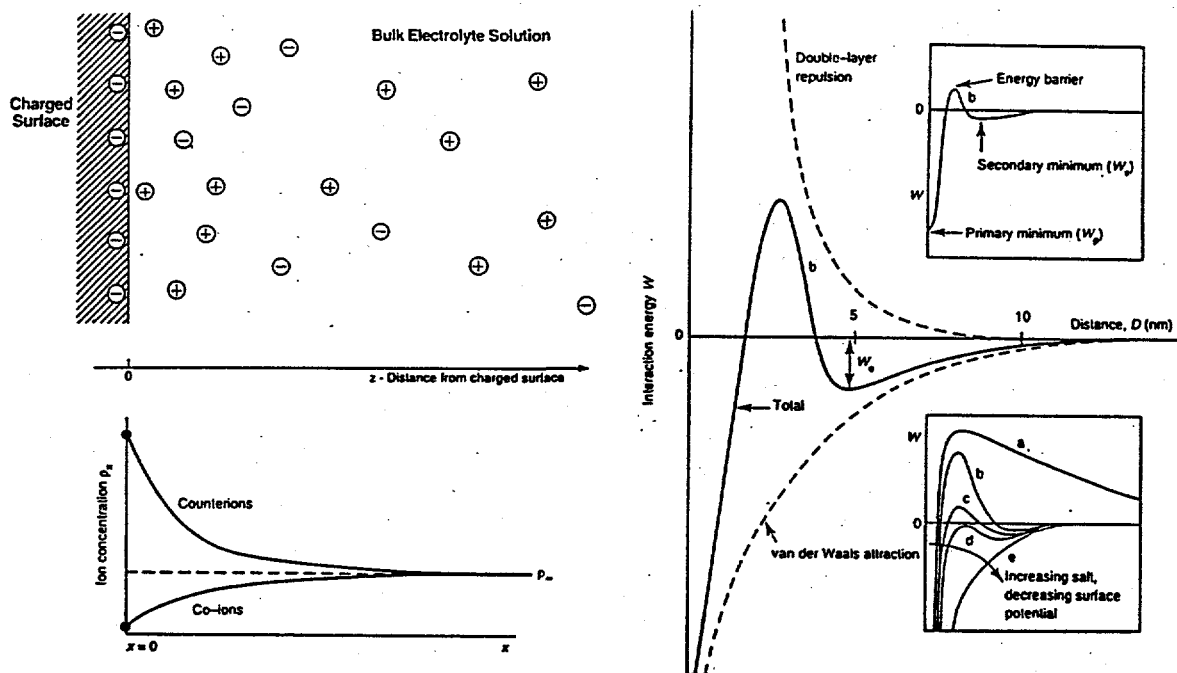


Figure 7.2. Electrical Double Layers. Particle behavior changes from repulsive to attractive as double layer repulsion decreases. Van der Waals attraction dominates when surface charge is low (near isoelectric point) or when salt collapses the electrical double layer.

dilute electrolyte solutions. The ionic clouds can repel each other, making the particle suspensions resistant to agglomeration. However, the ionic clouds collapse to being near the surface in solutions having a high salt content. When the double layer collapses, the particles can approach each other to the point where the van der Waals attraction overcomes the double layer repulsion, and the particles again form agglomerates.

The conditions leading to the formation of fixed charges on the particle surface need to be established to predict the extent of agglomeration. For this work, surface charge has been measured as a function of pH using electrophoretic mobility measurements (both alternating and direct current). The surface charge measurements (Figure 7.3) show that boehmite has an isoelectric point (pH at which the surface is neutral) of between pH 8.5 and 9.0. Below pH 7, the surface has a substantial positive charge, while above pH 10, the surface has a substantial negative charge.

The effect of surface charge on agglomeration has been determined for boehmite suspensions by measuring the agglomerate size distribution using light scattering techniques (Figure 7.4). For boehmite, the particles are completely dispersed near pH 3 (all particles are positively charged), leading to an agglomerate size almost identical to the primary particle size of 50 nm. At pH 7 (near the isoelectric point), the particles have little surface charge, and the primary particles stick to each other to form large agglomerates (50 μm). At pH 13, primary particles might be expected, since all particles are negatively charged. However, the particles are somewhat agglomerated (around 1 μm in size) due to the high salt content (0.1 M NaOH) of the pH 13 solution. In terms of tank waste processing, the agglomeration study shows particle interactions that control the properties to be discussed below can be turned on and off by changes in solution chemistry. In addition, the results show that, in the absence of TEM data, particle size distributions are of limited utility, since such distributions normally probe agglomerate sizes and not primary particles sizes. As will be shown below, agglomerates and primary particles having similar sizes do not exhibit similar properties.

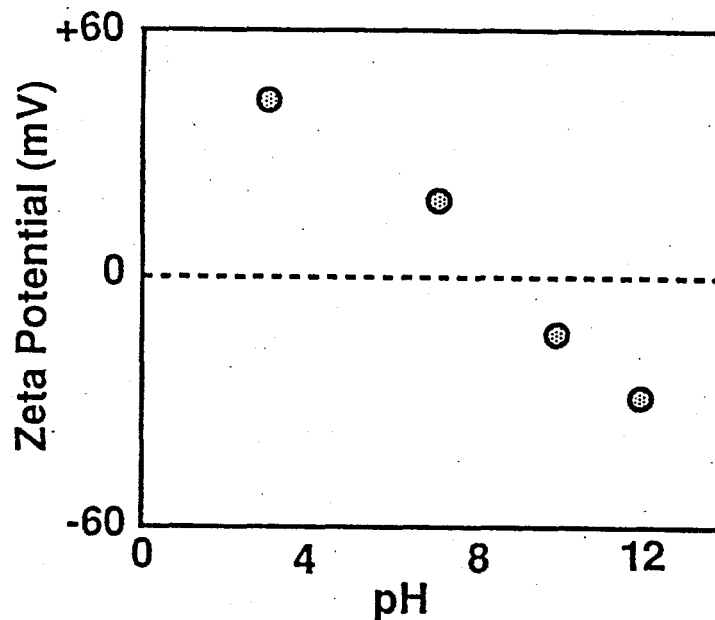


Figure 7.3. Surface Charge of AlOOH

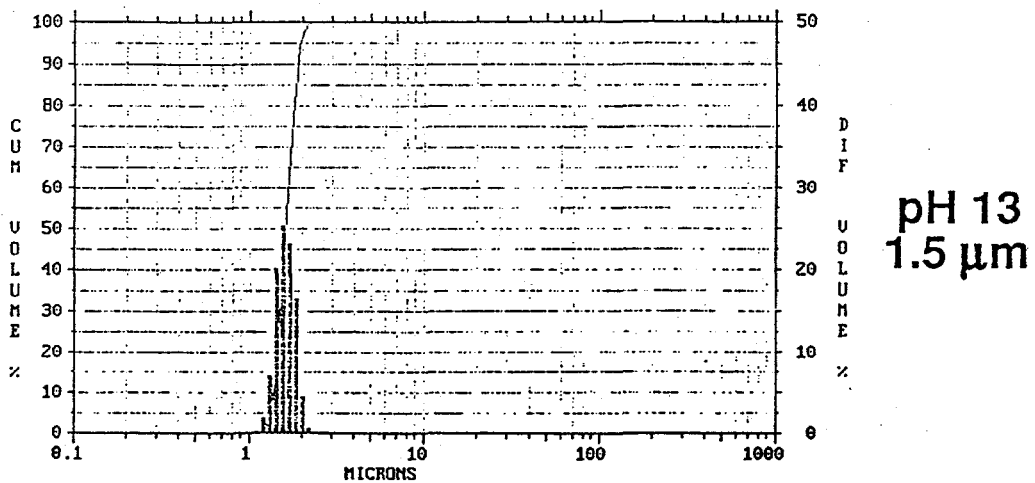
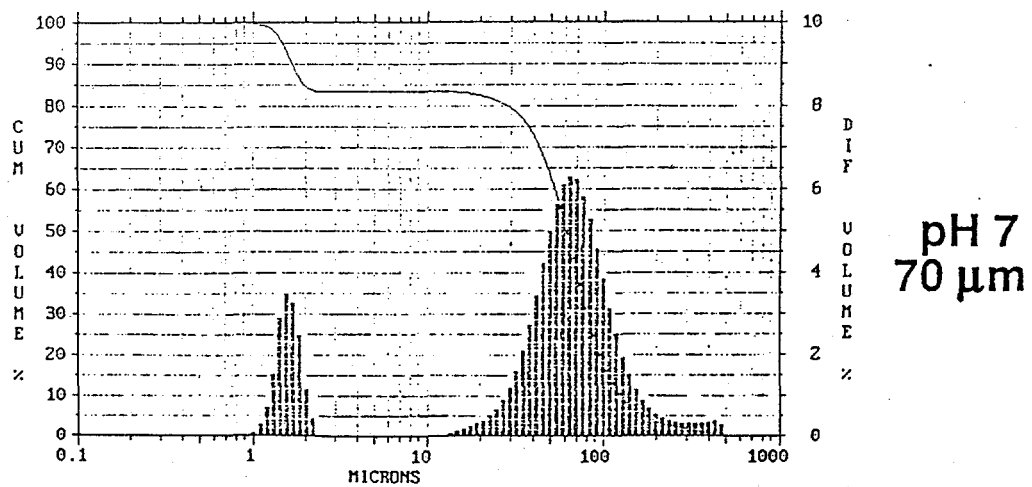
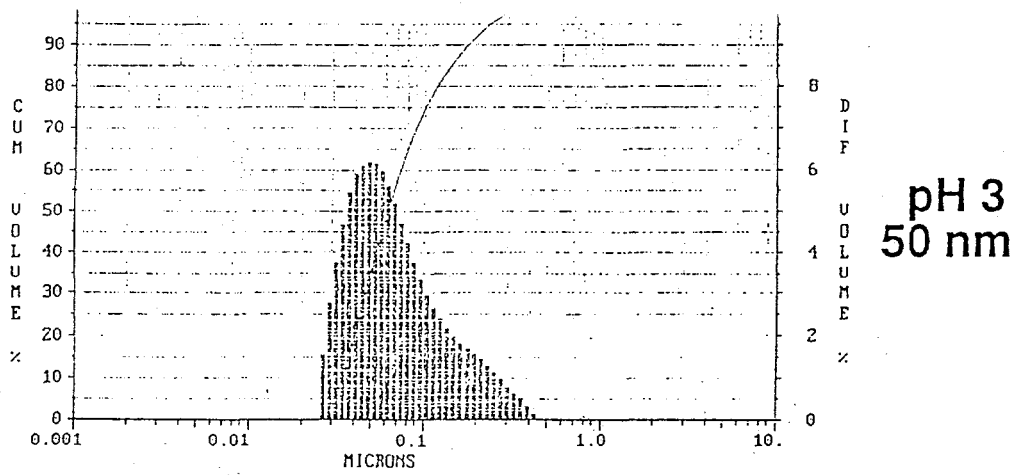


Figure 7.4. Boehmite (AlOOH) Agglomeration vs. pH. Solids loading, pH, and ionic strength (salt content) all influence agglomeration.

7.1.2 Viscosity Measurements

For retrieval and transport processes, the main processing goal is the ability to produce low viscosity solutions (< 60 cp) having the highest possible solids loadings of suspended particles. Low viscosity suspensions are required to ensure that fluids can be pumped and that transfer lines are not plugged. High solids loadings are required to minimize the volume of waste generated. Ideally, solids loadings as high as 30 or 40 vol% are desired. Studies are in progress to determine the viscosity behavior of both individual sludge components and mixtures of components. The purpose of these studies is to evaluate whether the goal of low viscosity, high solids loading sludge slurries can be met. To date, most results on slurry viscosity have been obtained on boehmite (AlOOH) suspensions, with limited studies being performed on gibbsite [$\text{Al}(\text{OH})_3$].

The viscosity of colloidal suspensions depends on the size, shape, solids loading, and interactions between the particles. For perfectly spherical, non-interacting particles, theoretical calculations (see Section 7.2) predict that the viscosity should increase with solids loading but that viscosities should stay below 50 cp even at solids loadings as high as 50 vol%. For boehmite, individual primary particles are non-interacting and are not agglomerated at pH 3 (see Section 7.1.1). At pH 3, viscosity measurements on boehmite suspensions (Figure 7.5) are consistent with the behavior predicted for

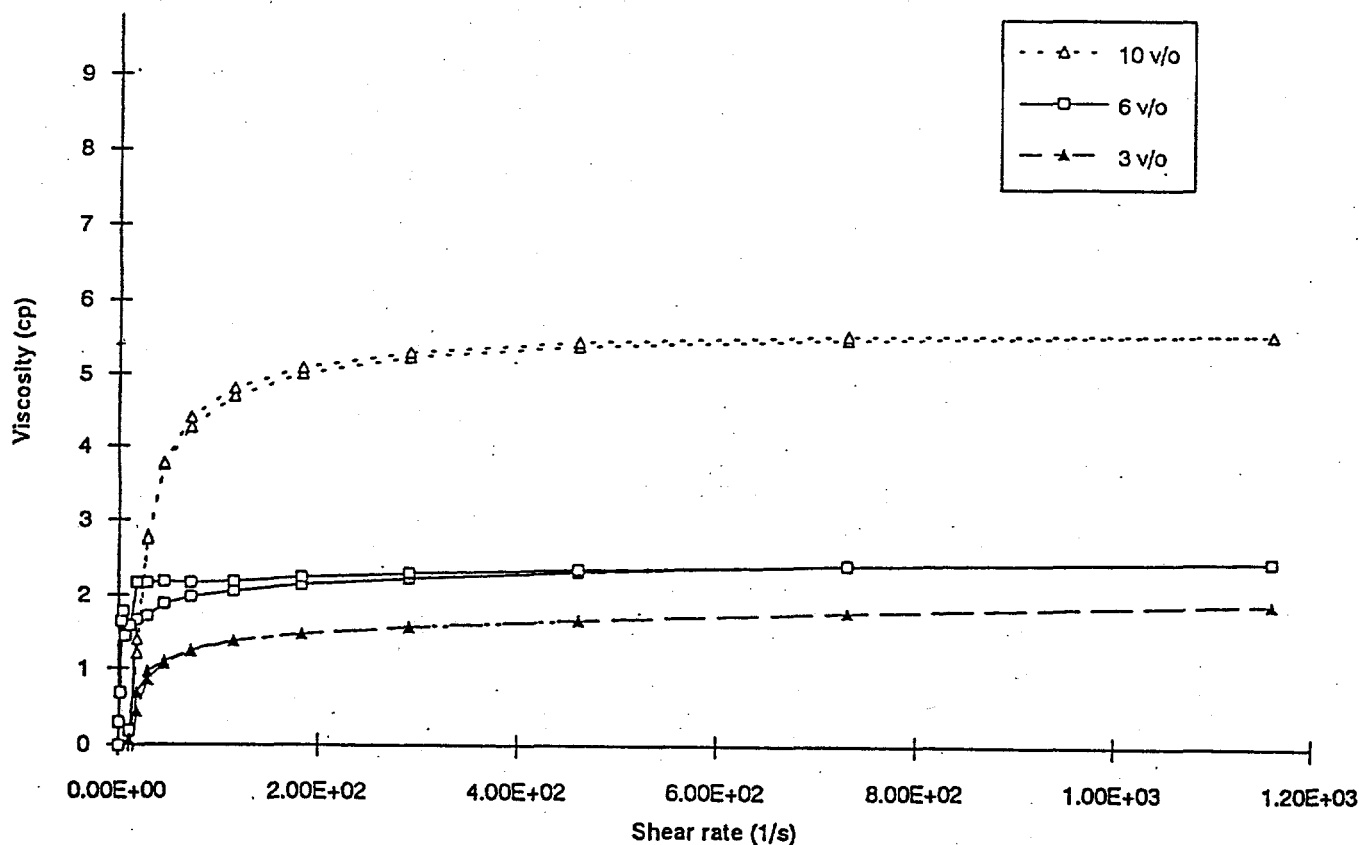


Figure 7.5. Viscosity of Dispersed Boehmite Suspensions. Conditions: pH 3, 0.01 M NaNO_3 , stir 2 h.

non-interacting particles. Up to at least 10 vol%, the boehmite suspensions have low viscosities (< 5 cp) and are Newtonian liquids (i.e., the viscosity is independent of shear rate). Such suspensions of non-agglomerated particles would be well suited for transport during waste processing.

The viscosity behavior of agglomerated boehmite suspensions is in sharp contrast to the behavior observed at pH 3. For example, at pH 10 (Figure 7.6), the viscosity of a 10 vol% suspension exceeds 10,000 cp at low shear rates (below 20 s⁻¹). The agglomerated slurries are non-Newtonian shear-thinning liquids. As the shear rate increases, interactions between the agglomerated particles leading to high viscosities can be broken up, resulting in lower viscosities at high shear rates. The overall viscosity versus shear rate curve can be fit by a classical power law curve of the form: shear stress = $\eta_0(\text{shear rate})^n$. Values for η_0 and n have been calculated for each slurry, allowing the solution viscosity to be predicted for any shear rate.

The effect of pH and ionic strength on slurry viscosity is illustrated in Figure 7.7, where solid points represent data collected to date and curves represent behavior expected for the suspensions. Agglomeration is expected to lead to high viscosity near the isoelectric point of AlOOH near pH 9. Viscosity is also expected to be high in strong acids or bases (pH below 2 or above 12) as a result of ionic strength effects that collapse the electrical double layer. Regardless of pH, high ionic strength solutions are expected to lead to agglomeration and high viscosities. For example, addition of sodium nitrate to the stable slurries produced at pH 3 quickly changes the solution from a Newtonian liquid with a low viscosity (below 5 cp) to a solid gel having a viscosity that is difficult to measure.

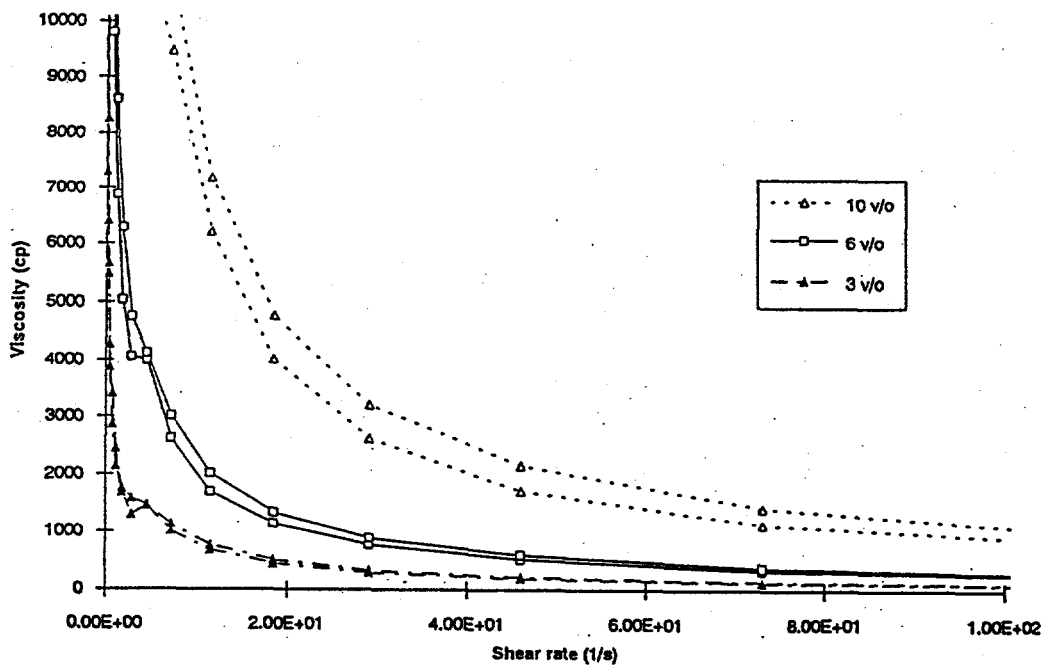


Figure 7.6. Viscosity of Agglomerated Boehmite Suspensions. Conditions: pH 10, 0.01 M NaNO₃, stir 2 h. All data exhibit power law behavior: shear stress = viscosity x (shear rate)ⁿ.

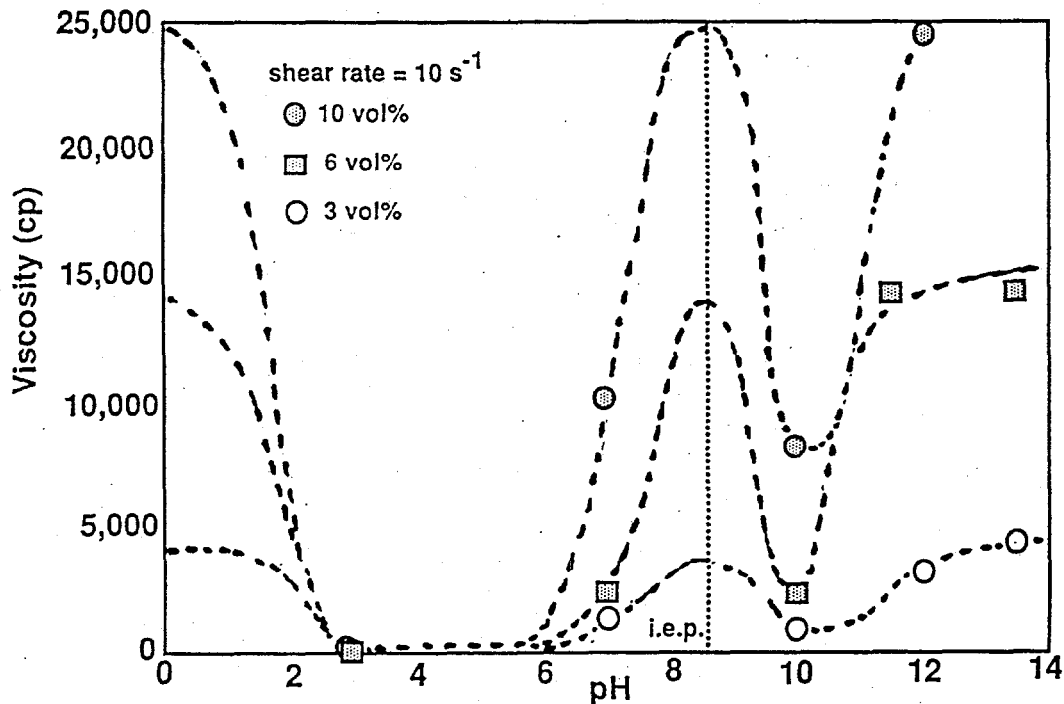


Figure 7.7. Boehmite Viscosity vs. pH. Electrostatic repulsions are overcome near the isoelectric point and in high ionic strength ($< 0.01 \text{ M}$) solutions.

The pH and ionic strength studies are critical in the context of tank waste processing. Most sludge slurries are expected to be basic (above pH 12) and to have high salt content (as high as 5 M NaNO_3). Such conditions are expected to suppress electrostatic stabilization of tank colloids regardless of chemical composition. If fine particles are present, viscous shear-thinning liquids are to be expected even for solids loadings as low as 3 vol%.

Limited viscosity measurements on gibbsite solutions (Figure 7.8) indicate that the high viscosity slurries are to be expected predominantly when substantial quantities of submicron particles are present. At 4.2 vol%, and in 1 M NaOH (where agglomeration is promoted), gibbsite slurries having primary particle sizes of 10, 1, and $0.25 \mu\text{m}$ exhibit moderate viscosities (below 20 cp) at a shear rate of 115 s^{-1} . This appears to be related to the degree of agglomeration, which is lacking in the large particles but is pronounced for the small particles (see Section 7.1.3).

A final observation with regard to viscosity is that kinetic effects are apparent in viscosity data. The viscosity is sensitive to parameters such as storage time (Figure 7.9) and mixing. Agglomerate structures are not established instantaneously but can evolve over a period of hours or even days. For example, at pH 3, a stabilized solution of particles in a 10 vol% slurry can form a viscous gel over a period of several days. Gel formation has been observed at solids loading as low as 3 vol%.

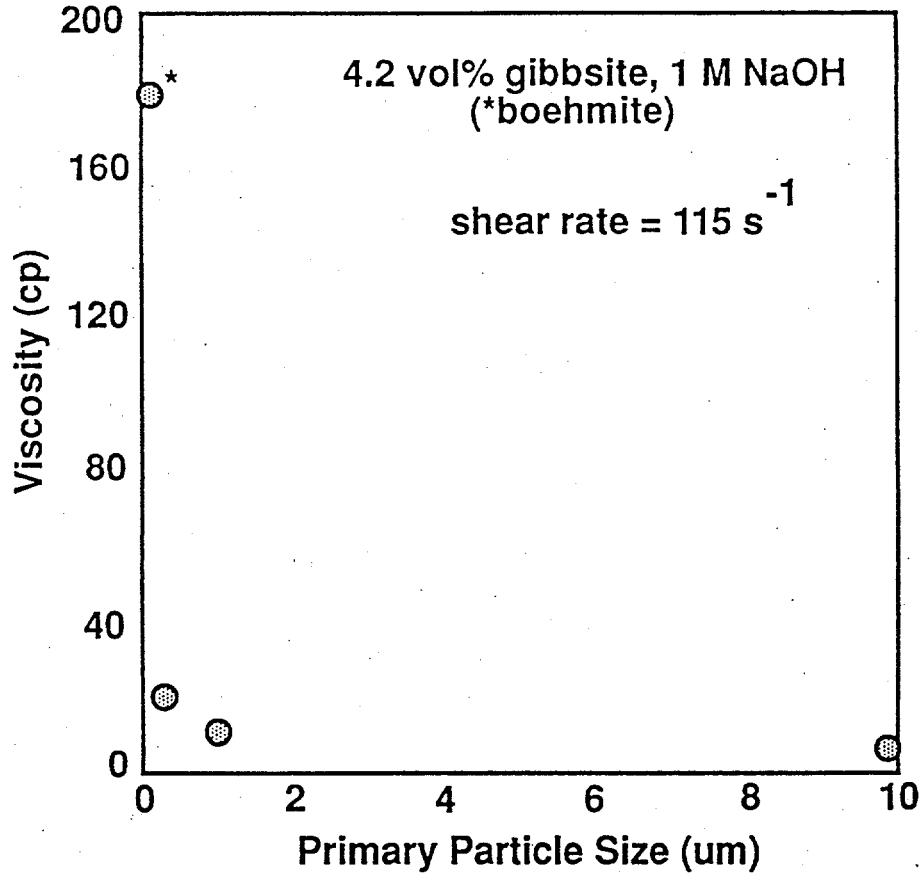


Figure 7.8. Viscosity vs. Primary Particle Size. Agglomeration and viscosity increase dramatically as particle size drops below $1 \mu\text{m}$.

Early results on retrieval and transport include the following implications:

- Slurry viscosities are sensitive to a wide range of parameters, including solids loading, pH, salt content, age of suspension, shear rate, and degree of agitation.
- Low viscosity ($< 100 \text{ cp}$) Newtonian fluids can be produced from colloidal slurries of tank sludge components such as gibbsite and boehmite if the individual crystallites (or primary particles) are larger than about $1 \mu\text{m}$. Solids loadings of at least 10 vol% are possible for slurry transport, consistent with baseline processing assumptions.
- Low viscosity fluids can also be produced for submicron slurries if the particles are dispersed rather than agglomerated. For boehmite, dispersed fluids form between pH 3 and pH 5 in solutions having low salt content ($< 0.01 \text{ M NaNO}_3$).

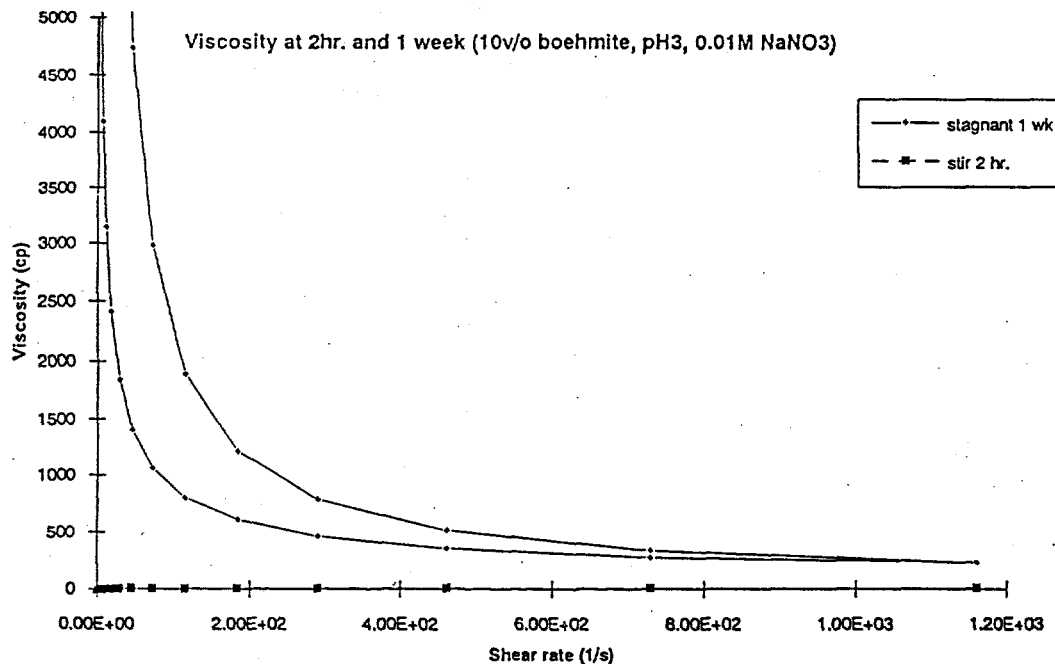


Figure 7.9. Viscosity of Boehmite Suspensions vs. Sample History. Viscosity at 2 hr and 1 week (10 vol% boehmite, pH 3, 0.01 M NaNO₃).

- When submicron particles agglomerate, the resulting suspensions can exhibit viscosities in excess of 25,000 cp and can gel even at solids loadings as low as 3 vol%. Agglomeration is promoted in the high pH, high salt content solutions expected to be representative of tank wastes. It is currently unknown how dilute the particle suspensions must be to prevent viscosity problems in such slurries, but a dilution of tank waste by factors of over 100 is not unrealistic for producing a pumpable liquid.
- Agglomerated suspensions are shear thinning liquids. If solutions are agitated, as in mixing and pumping operations, interactions between agglomerates can be broken up to the point where substantial decreases in viscosity can be observed. However, fluids must be kept moving. For example, if pumping ceases during transport, high viscosities will be quickly reestablished, and viscous gels will foul the transfer lines.

7.1.3 Sedimentation and Centrifugation

The baseline process envisions that once sludges have been retrieved and transported to a processing facility, collected sludges may be stored in holding tanks. Washing and leaching solutions may also be added to the tanks to help minimize the solids inventory in the HLW stream. For all in-tank processes, the baseline process for solid-liquid separations involve settle-decant steps in which the solid particles are expected to sink to the bottom of the tank, leaving behind a particle-free supernatant liquid that can be pumped off and sent into the LLW stream. Desired characteristics of the settle-decant steps are that the process be relatively rapid (sedimentation rates of around 3 cm/hr are desired); that the resulting sediment be compact, allowing most of the liquids in the tank to be

removed; and that few particles remain in suspension that might either contaminate or foul equipment in the LLW processing stream. Since sedimentation represents a key step in the baseline process, experiments are being conducted to determine the key factors controlling sedimentation, starting with model gibbsite and boehmite suspensions.

The simplest expression providing estimates for sedimentation rates is Stokes' Law, which describes how quickly spherical, non-interacting particles should sink under the force of gravity:

$$V = 2gr^2(\rho_1 - \rho_2)/9\eta \quad (7.1)$$

where g is the force of gravity, r is the particle radius, ρ_1 and ρ_2 are the densities of the particle and the fluid, respectively, and η is the solvent viscosity ($= 1$ cp for water). Using Stokes' Law, initial sedimentation rates for particles such as boehmite and gibbsite can be calculated. The calculations indicate that primary particles of gibbsite or boehmite should settle rapidly (> 200 cm/hr) if the particles are larger than $100 \mu\text{m}$. Particles with a $10\text{-}\mu\text{m}$ radius should settle at a rate of approximately 2 cm/hr; $1\text{-}\mu\text{m}$ particles hardly settle at all (0.02 cm/hr); and submicron particles stay in suspension indefinitely (no sedimentation).

Experimental sedimentation velocities have been measured for 0.25- , 1- , and $10\text{-}\mu\text{m}$ particles of gibbsite as well as $50\text{-nm} \times 5\text{-nm}$ boehmite plates. Sedimentation velocities have been determined in 4.2 vol% suspensions in 1 M NaOH by pouring suspensions into clear cylinders and then watching the position of the boundary between the clear supernatant liquids and the settling sediment as a function of time. Results of the sedimentation experiments (Figure 7.10) can be used to determine initial sedimentation rates, probe how sedimentation rates decrease as the sediment becomes more compact (see Section 7.2), and (at long times) provide information concerning final sediment densities (vol% particles in the sediment bed). Initial sedimentation velocities have been compared with the predictions of Stokes' Law (Table 7.3). The results indicate that the $10\text{-}\mu\text{m}$ gibbsite particles sink at about the rate predicted from Stokes' Law (2 cm/hr), indicating that the particles have not undergone much agglomeration. As expected, the smaller primary particles sink much slower than the $10\text{-}\mu\text{m}$ particles. However, the sedimentation velocities are much greater than expected for the primary particles, indicating that the particles are heavily agglomerated. The observed sedimentation velocity can be used to provide an estimate for agglomerate sizes that are in qualitative agreement with the limited agglomerate size measurements performed to date. For example, the 50-nm boehmite particles exhibit an effective agglomerate size of approximately $0.6 \mu\text{m}$, meaning that each agglomerate contains roughly $20,000$ primary particles.

Even with extensive agglomeration, sedimentation velocities for the submicron particles are too slow to meet the current guidelines for settle-decant operations. Instead of the desired 3 cm/hr sedimentation rates, the sedimentation velocity for the agglomerated submicron boehmite particles is 0.002 cm/hr in 1 M NaOH. When the boehmite particles are dispersed, no sedimentation is observed whatsoever. In fact, no sedimentation is observed for dispersed boehmite even when suspensions are placed in a centrifuge at $20,000$ times the force of gravity. The centrifugation results illustrate how solution parameters that promote good transport (i.e., low viscosity suspensions containing dispersed particles) can result in production of solutions that are completely unacceptable from the standpoint of settle-decant operations.

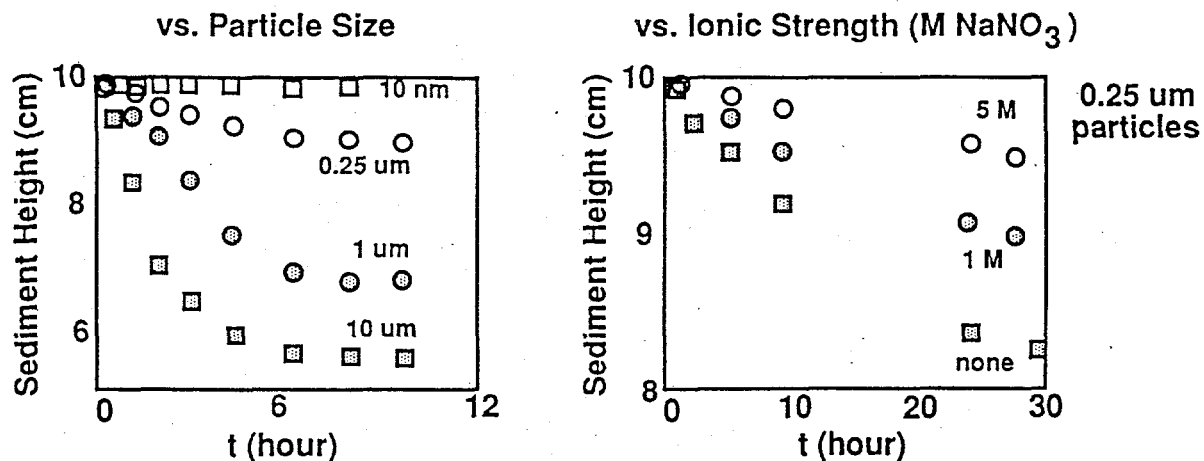


Figure 7.10. Gibbsite Sedimentation Rates. Conditions: 4.2 vol% suspensions, 1 M NaOH, 10-cm column. Large particles settle fastest; smallest particles do not settle. Agglomeration induced at high ionic strength promotes sedimentation.

Table 7.3. Gibbsite Sedimentation Rates. Sample Conditions: 4.2 vol% (initial), 1 M NaOH.

Primary Diameter	Calculated Sedimentation	Measured Sedimentation	Calculated Diameter	Cake Density
10 μm	0.5 cm/hr	2 cm/hr	19 μm	17 vol%
1 μm	0.005 cm/hr	0.6 cm/hr	12 μm	8.8 vol%
0.25 μm	0.0003 cm/hr	0.15 cm/hr	6 μm	5.0 vol%
0.05 $\mu\text{m}^{(a)}$	2.2×10^{-6} cm/hr	0.002 cm/hr	0.6 μm	no settling

(a) Boehmite.

Centrifugation at 20,000 G has been used to accelerate the rate of settling of agglomerated boehmite suspensions. Although sedimentation rates have not yet been measured in the centrifuge, the centrifuge does compact the sediment much more rapidly and completely than gravity and allows us to estimate sediment cake densities. For boehmite, it appears that the final sediment density for the agglomerated material ranges from 25 to 30 vol%, independent of agglomerate size.

The impact of sediment cake densities on settle-decant steps is illustrated in Figure 7.11. In an ideal settle-decant step, all particles would sink to the bottom after mixing to form a highly compact solid mass containing little interstitial liquid. For a 10-vol% slurry, sedimentation of monodispersed spheres could form a solid layer filling only 14% of the tank volume in which 74 vol% of the material in the layer is particles, and 26 vol% is interstitial liquid. Of the total liquid in the tank, 96% would be supernatant liquid that could be removed by pumping, while only 4% of the total liquid would remain

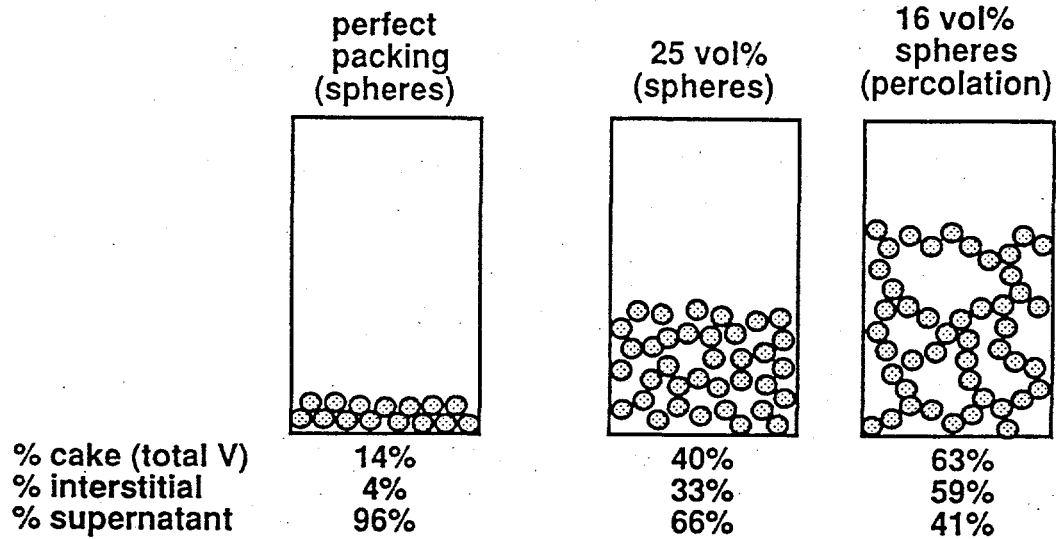


Figure 7.11. Impact of Agglomeration on Settle-Decant Steps. Example: 10 vol% slurry.

as interstitial liquid. For such a system, solid-liquid separations via settle-decant processing is highly efficient. However, if final sediment densities are 25 to 30 vol%, as seen experimentally, then the final sediment can occupy roughly half of the total tank volume and contain roughly 1/3 of the total liquid present in the tank. For this case, the solid-liquid separation step can only remove 2/3 of the tank liquids, leading to an inefficient separation. In extreme cases, where the suspended particles form a gel, there are no supernatant liquids, and there can be no solid-liquid separations. Therefore, the nature and extent of sedimentation is critical to an evaluation of settle-decant steps.

7.1.4 Pressure Filtration Studies

Once settle-decant operations are deemed complete, and the supernatant liquids are removed, it is inevitable that some particles will be retained in the liquid phase. It is also inevitable that the remaining particles will represent the fraction of particles that are the smallest. The small remaining particles are of concern because they could represent radioactive contaminants in the LLW stream and because such particles could foul processing units such as ion exchange columns that are part of the LLW processing stream. The primary solid-liquid separation process included in the LLW baseline involves filtration. For this reason, filtration studies are being conducted on the same colloidal suspensions under study in the viscosity and sedimentation experiments.

The primary tool used to date in filtration studies is a pressure filtration system. The simplest equation describing the filtration process in such a unit is Darcy's Law:

$$dV/dt = KAP\eta L \quad (7.2)$$

where dV/dt is the filtration rate (volume/hr), K is the permeability of the filtration medium (in this case, the as-deposited filter cake), A is the surface area of the filter, P is the applied pressure, η is the solution viscosity, and L is the thickness of the filtration medium (or filter cake). Under normal filtration conditions, the maximum pressure difference across the filter cake would be a vacuum of 1 atm, or 14 psi. However, our pressure filtration unit is capable of pressures exceeding 6000 psi (or approximately 400 atm). The high-pressure capability means that liquids can be forced through filter cakes even if they are relatively impermeable. Filter cakes are trapped on a 1-mil-thick filtration membrane having desired porosity. For most experiments described below, filtration was performed on a membrane containing 0.2- μm pores. The filtration results provide information concerning filtration rates as well as filter cake permeabilities.

The high-pressure capability of the pressure filtration unit has proven to be critical for studying the filtration of boehmite suspensions. If the particles are dispersed and are small relative to the pores in the filtration membrane, the particles penetrate the membrane and solid-liquid separations are not achieved. However, on the 0.2- μm membrane, a thin layer of boehmite soon forms on the membrane that has pores smaller than the primary particles. Boehmite particles do not pass through the boehmite filter cake, which thickens as a function of time. As the boehmite cake thickens, the rate at which fluid can be forced through the membrane decreases. The volume of solution passing through the filter is linear as the square root of time in most experiments (Figure 7.12). An analysis of data, such as shown in Figure 7.12, can be used to estimate the thickness of the filter cake with time and to calculate the permeability of the filter cake.

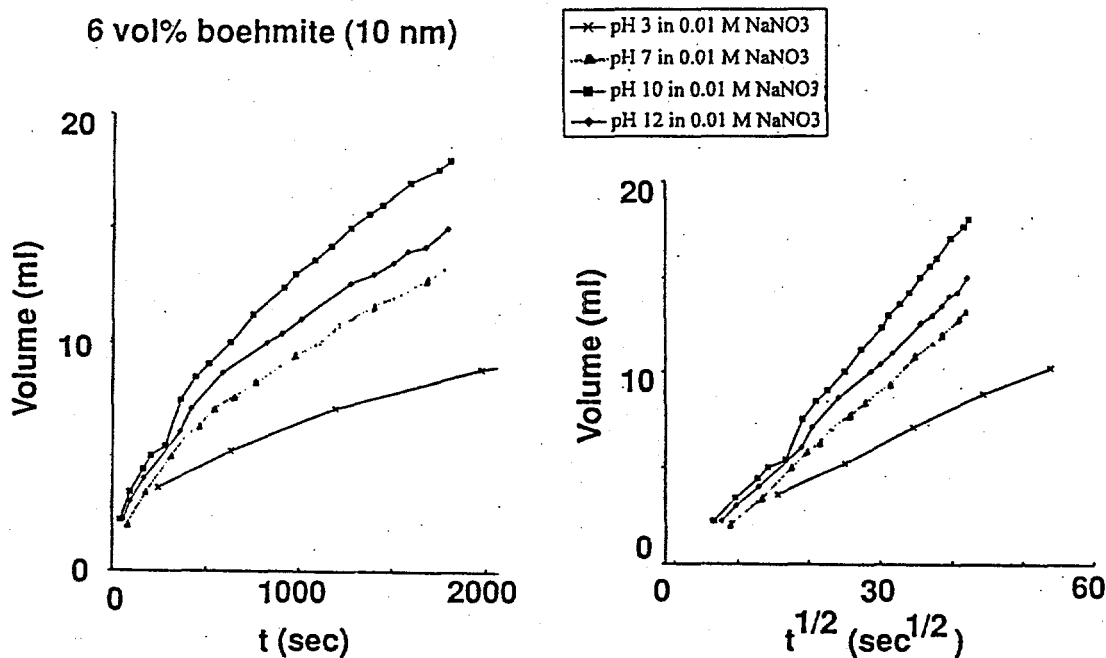


Figure 7.12. Filtration Rates vs. Time

The pressure filtration results indicate that suspensions of boehmite particles form highly impermeable filter cakes regardless of the degree of particle agglomeration (Figure 7.13). Permeabilities are lowest for cakes formed from dispersed boehmite, which can presumably pack more efficiently than agglomerates. The measured permeability of approximately 10^{-21} m^2 is what would be seen for a 1-mm-thick filtration membrane having pores approximately 0.5 nm in diameter. Increases in agglomeration at high pH are accompanied by an increase in permeability by a factor of about 100, but even these permeabilities are exceedingly low. Given the low filter cake permeabilities, it is perhaps surprising that measured solid densities of the filter cakes are all approximately 20 vol% solids, independent of the degree of particle agglomeration.

To put the measured permeabilities in perspective, if the desire for a filter is to have liquid levels above the filter membrane drop at a rate of 1 cm/hr, the maximum allowed thickness of the most permeable boehmite cake examined to date would be approximately $0.1 \mu\text{m}$. Thicker cakes would foul the filter. If the desire is to filter a column of water 1 m high above the membrane, the maximum boehmite loading that could allow the entire volume to be filtered without fouling is $10^{-5} \text{ vol}\%$. Therefore, the pressure filtration studies suggest that if submicron particles are present, normal filtration is not a viable option for solid-liquid separation. The problems associated with filtering fine particles have been recognized in the baseline process, which is why alternate filtration schemes such as cross-flow filtration with back-pressure pulsing are under consideration. However, careful investigations will be required to determine whether the alternate filtration schemes alleviate the serious problems posed by submicron particles.

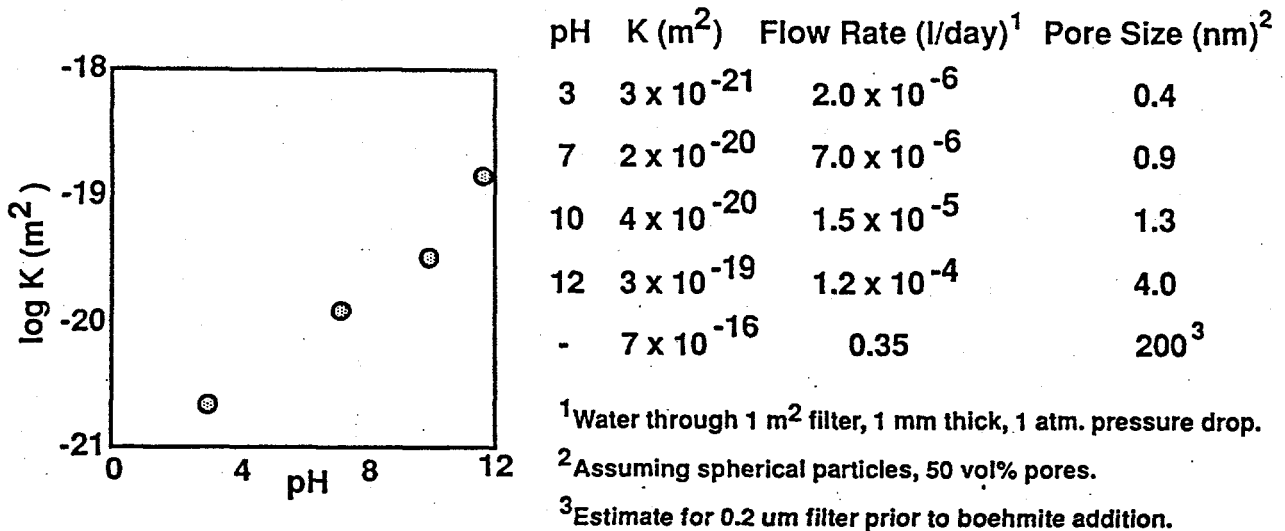


Figure 7.13. Permeability of Boehmite Filter Cakes. Permeability increases as boehmite agglomeration increases. Filter cakes are impermeable when primary particles are small (10 to 20 nm). Although impermeable, filter cakes have low packing densities (25 vol%).

7.2 Modeling Studies

As the experimental results clearly indicate, a large number of factors play a role in determining the rheological and sedimentation properties of colloid suspensions. Particle size distributions, surface charge, short-range interparticle forces, hydrodynamic interactions, chemical conditions, and electric fields can all influence tank waste processing conditions. Given the large diversity of waste types present at the Hanford Site, it is important to understand the physical principles governing the behavior of both real sludge and the simpler sludge simulants used in experimental studies such as those described above. While the simple equations outlined in 7.1 can provide a qualitative appreciation of major factors that control waste processing, more detailed models are required if realistic predictions of sludge behavior are to be made.

The purpose of the colloidal modeling activity is to provide the theoretical and analytical tools required for interpreting the data obtained in the colloidal experimental tasks, and to eventually predict the behavior of colloidal systems encountered in tank waste processing. Efforts thus far have focused on the development of computational tools which model the basic physics of colloidal systems. The initial calculations have been performed on simple suspensions of monodispersed spheres. Once the simple system is understood, features can be added to make the models more representative of real wastes by including different particle types and interparticle interactions. The computational tools currently under development include a Stokesian Dynamics model, a Monte Carlo sedimentation model, and a finite-difference transient sedimentation model.

7.2.1 Stokesian Dynamics Model

A computer program based on the Stokesian Dynamics method has been developed which can simulate the concerted motions of many solid particles suspended in a fluid medium. Particles in suspension may interact through hydrodynamic, Brownian, colloidal, interparticle, or external forces. The simulation technique involves temporal integration of the equations of motion to find the instantaneous positions and orientations of the suspended particles. Forces between the particles are configuration-dependent and are updated with each step. Even though the Stokesian Dynamics method is only 10 years old, it has already been applied to problems of sedimentation, flocculation, and diffusion and transport in porous media.

Figure 7.14 shows that Stokesian Dynamics calculations provide exact fits to experimental data for viscosity versus solids loading of non-interacting monodispersed hard spheres with purely hydrodynamic forces. The increase in viscosity at higher solids loadings is due to particle clustering resulting from lubrication forces between adjacent particles. As mentioned in Section 7.1, such calculations indicate that for ideal, non-interacting suspensions, slurry viscosities below 60 cp can be achieved even at solids loadings as high as 50 vol%. Future calculations will incorporate interparticle interactions and particle mixtures to attempt to simulate the behavior of the shear-thinning agglomerated systems seen in the experimental studies at high pH.

Another potential application of Stokesian Dynamics is the calculation of sedimentation velocities. As mentioned in Section 7.1, while Stokes' Law can provide information concerning initial sedimentation velocities for non-interacting spheres, it does not indicate how sedimentation rates might change as particles settle to the point where they become concentrated and begin to interact with each other. Figure 7.15 summarizes Stokesian Dynamics results showing that sedimentation velocities are expected

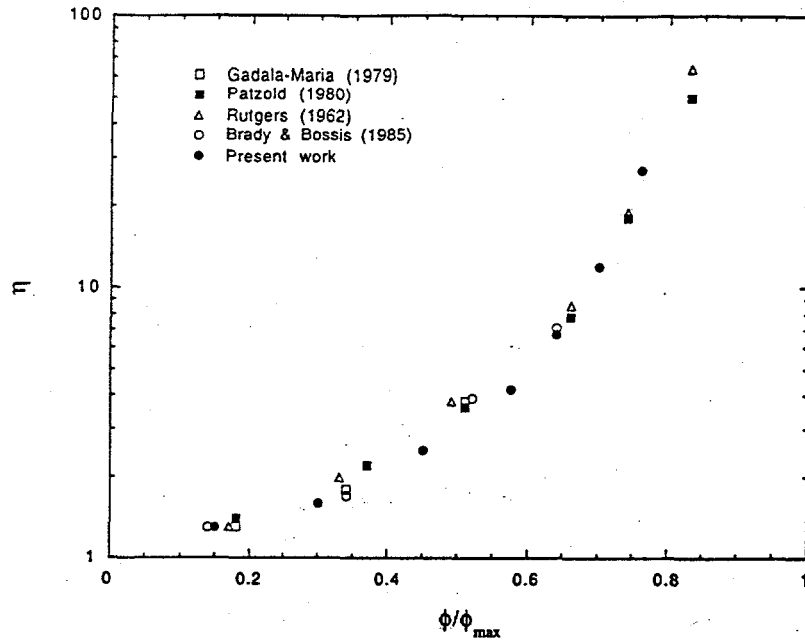


Figure 7.14. Relative Viscosity as a Function of Volume Fraction

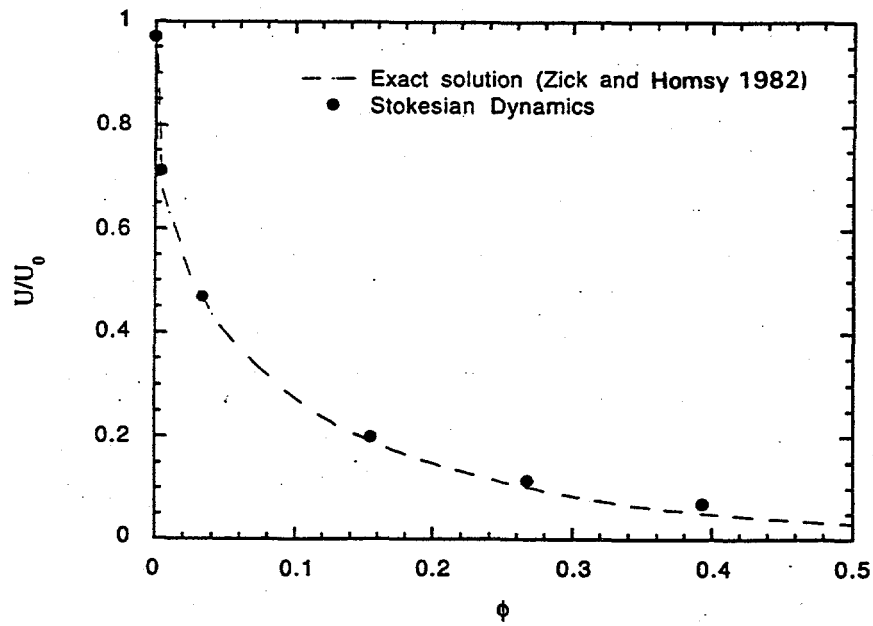


Figure 7.15. Relative Sedimenting Velocities of a Cubic Array of Hard Spheres as a Function of Volume Fraction

to decrease dramatically as the volume fraction occupied by particles increases during settling. The results are identical to those obtained via analytical solutions. Although experimental results obtained to date are for agglomerated suspensions, the general shape of experimental sedimentation curves (Figure 7.10) match calculated trends. Direct comparisons between theory and experiment will be possible once interparticle interactions and particle mixtures are included in the sedimentation simulations.

7.2.2 Sedimentation Equilibrium Model

The final equilibrium thickness and density distributions in sediments are important in determining the overall efficiencies of settle-decant operations. A Monte Carlo model developed by Biben et al. (1993) is being adapted to consider sludge sedimentation to determine density profiles on concentrated colloidal suspensions in sedimentation equilibrium. The model relates particle size, solid density, interfacial chemistry, and interparticle interactions to sedimentation properties. The model calculates the total potential energy of the particle system due to interparticle interactions and gravity, and then allows the particles to move to new positions. The calculations are performed tens of thousands of times until the calculated potential energy for the system reaches a minimum value corresponding to the most stable equilibrium configuration. Particle density profiles are then calculated for the entire sediment column.

Figures 7.16 and 7.17 depict equilibrium sediment profiles for monodispersed hard spheres as a function of effective temperature or particle density. The profiles show the relative density of particles with relative distance from the bottom (corresponding to $z^* = 0$) for two values of the effective gravitational length $\alpha = mgr/kT$, where m is the mass of the particle, g is the force of gravity, r is the particle radius, k is Boltzmann's constant, and T is temperature in K. The results show that doubling the particle mass (or decreasing the temperature by a factor of 2) results in sediments that show more structured particle layering or "crystallization" near the bottom. The lower density/higher temperature case (Figure 7.17) has a smoother profile with a "tail" that extends to a higher elevation (i.e., the sediment cake is thicker).

The sediment characteristics of particle mixtures are depicted in Figures 7.18 and 7.19. Figure 7.18 shows results for a system containing equal numbers of large and small particles ($r_1/r_2 = 0.5$) having the same density, and therefore different masses. Figure 7.19 shows sediments formed from large and small particles having the same masses but different densities (again with the ratio of particle radii equal to 0.5). When two sizes of the same particle type are present, the larger (and thus heavier) particles concentrate near the bottom (Figure 7.18). The light particles form a much less compact mass sitting on top. Such partitioning during settle-decant steps would result in a very thick sediment that would be more readily disturbed and resuspended during removal of supernatant liquids than would be the case for a homogeneous sediment. When particles having the same mass are present, the smaller particles concentrate near the bottom through excluded volume effects. In both cases, a high degree of particle partitioning is observed as a function of sedimentation. Such partitioning needs to be considered when evaluating settle-decant processing steps.

Work in the next quarter will begin to incorporate particle-particle interactions (van der Waals attractions and electrostatic repulsions) into the sedimentation equilibrium model. Once these particle interaction terms are included, the effects of solution chemistry (such as pH and ionic strength) can be explored. Sedimentation studies will also be expanded to include development of computational models

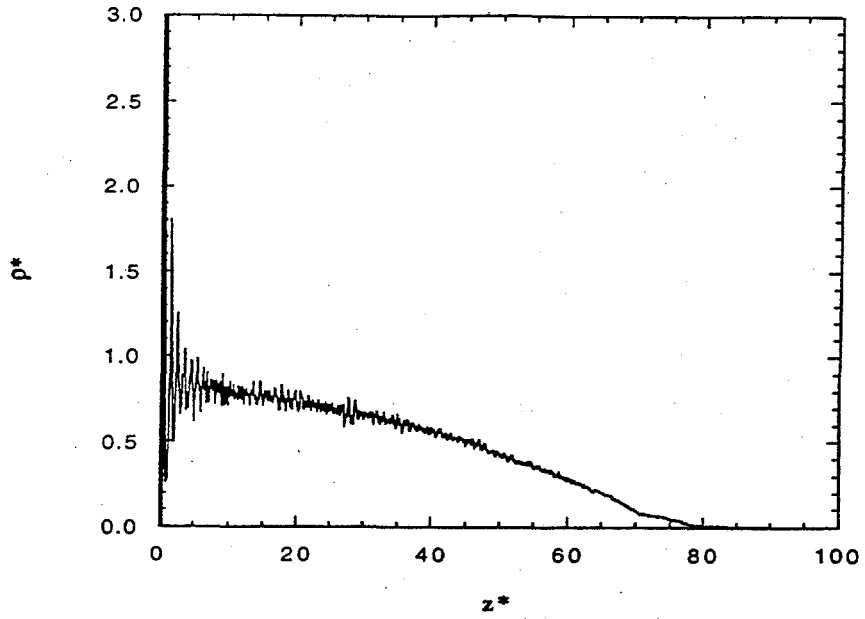


Figure 7.16. Reduced Density Profile of a Monodispersed Hard Sphere Suspension for $n_s^* = 40$ and $a^* = 0.2$

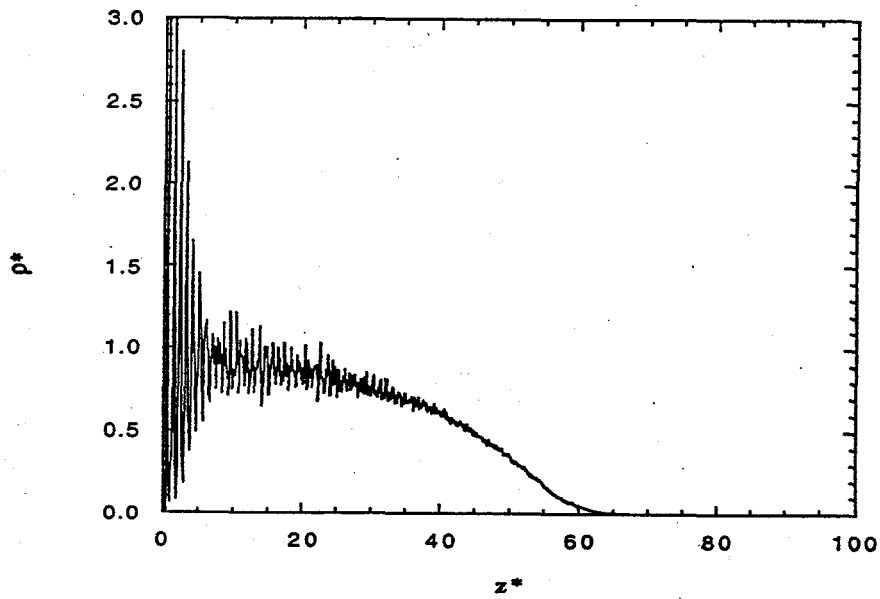


Figure 7.17. Reduced Density Profile of a Monodispersed Hard Sphere Suspension for $n_s^* = 40$ and $a^* = 0.4$

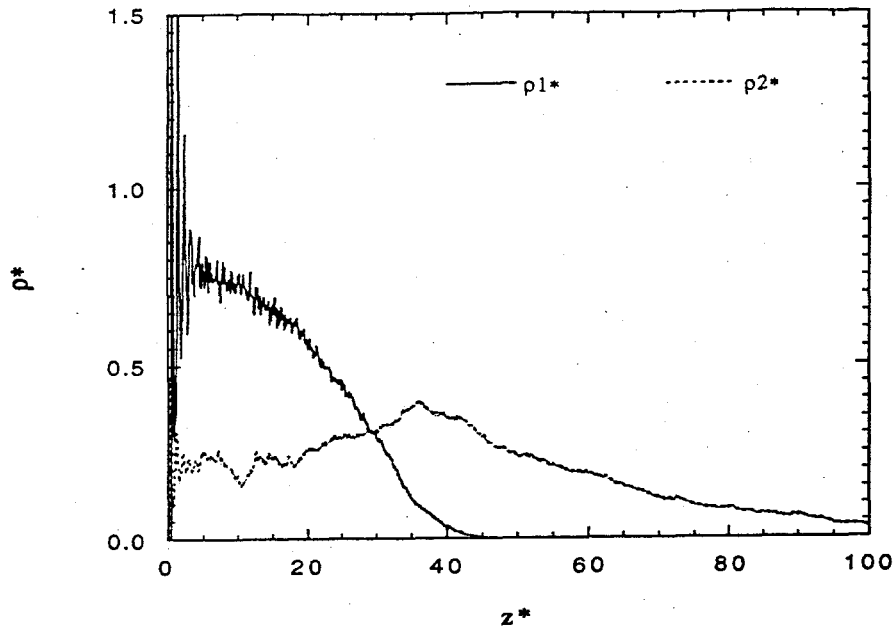


Figure 7.18. Reduced Density Profile of an Equimolar Binary Hard Sphere Suspension with Particle Size Ratio $\sigma_2/\sigma_1=0.5$ and Mass Ratio $m_1/m_2=(\sigma_1/\sigma_2)^3$ (equal density)

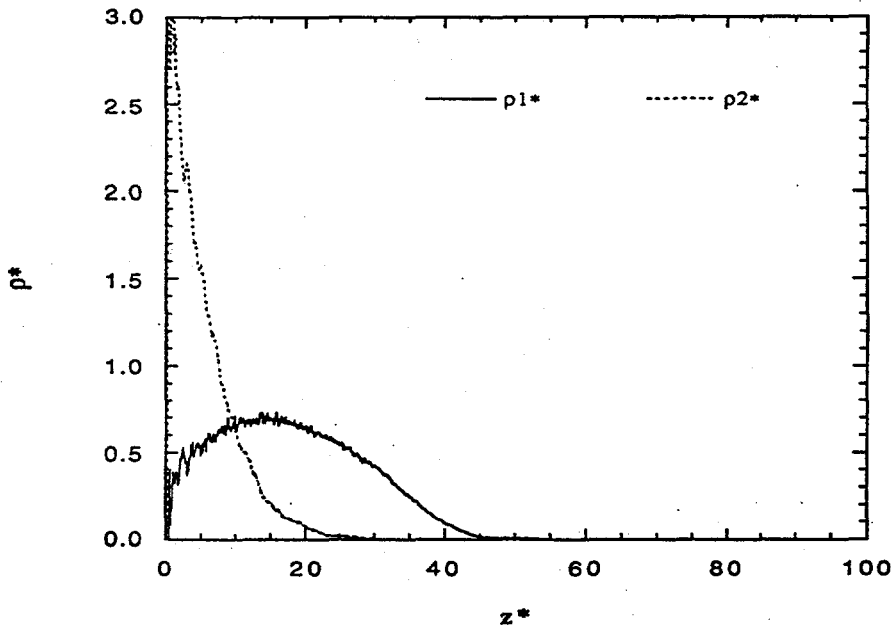


Figure 7.19. Reduced Density Profile of an Equimolar Binary Hard Sphere Suspension with Particle Size Ratio $\sigma_2/\sigma_1=0.5$ but for equal effective masses ($m_1=m_2$)

which describe the transient sedimentation and compaction behavior of particulate suspensions. The transient model will include hindered settling velocities, temperature-dependent diffusion, and osmotic pressure. The model will not only describe the sedimentation behavior in the bulk, but also the relative layering of different particle species and compaction of the sediment layer as a function of time.

7.3 Hot Colloids Laboratory

All measurements of colloidal properties carried out to date have involved studies of non-radioactive simulants. While the simulants contain particles similar to those identified in actual tank waste, work on simulants alone will never be sufficient to define sludge properties to the level required for process validation. While experimental and theoretical studies such as those outlined above can provide a sound technical basis for waste processing, the premises of the work on colloid chemistry must be tested on real sludge samples. For this reason, a Hot Colloids Laboratory is being established. The first hurdle to overcome in establishing the Hot Colloids Laboratory is to identify appropriate space to house the facility. Where possible, the laboratory will contain equipment similar to that housed in our cold facilities, but will be dedicated to handling samples of actual radioactive sludges. The laboratory will consolidate equipment used to support a range of tasks in the pretreatment project, including the TWRS Tank Waste Treatment Science and Sludge Treatment Technology tasks. Some equipment used for TWRS retrieval, transport, and safety projects also will be included.

7.4 Summary

Work is in progress to study properties of tank sludge components that are relevant to tank waste processing. To date, experimental work has focused on understanding properties of simple boehmite and gibbsite suspensions as a function of particle size and shape, solids loading, pH, and salt content. While it is too early to draw definitive conclusions, the work performed to date suggests the following:

- It appears that many of the current guidelines used in evaluating the baseline processes for solid-liquid separations are valid if the primary particles in sludge are larger than 10 μm in size. With large particles it is possible to achieve low slurry viscosities (< 60 cp) at high solids loadings (> 10 vol%) for retrieval and transport, to have reasonable initial sedimentation velocities (> 3 cm/hr) for settle-decant operations, and to achieve rapid filtration rates (> 1 cm/hr).
- The current processing guidelines do not appear to be valid if the bulk of the material to be processed consists of submicron particles. Fine colloidal particles can form highly viscous ($> 25,000$ cp) shear-thinning liquids at solids loadings as low as 3 vol%, can form suspensions that exhibit negligible sedimentation velocities (either in the form of highly dispersed suspensions or as highly agglomerated gels), and can form impermeable filter cakes that will clog most filtration media.

At this point processing problems appear likely associated with submicron particles. It is too early to tell the extent to which large particles (or particle mixtures) might mediate the potentially harmful effects of the smaller particles, or what alternatives (involving either chemistry or equipment modifications) might be most effective in controlling desired solid-liquid separations when submicron particles

are present. However, future work with other major, single components in sludge; with component mixtures; and with solutions containing organics should help identify appropriate strategies for dealing with processing problems.

7.5 References

- Biben, T., J-P. Hansen, and J-L. Barrat. 1993. "Density Profiles of Concentrated Colloidal Suspensions in Sedimentation Equilibrium." *J. Chem. Phys.* 98:7330.
- Brady, J. F., and G. Bossis. 1985. "The Rheology of Concentrated Suspensions of Spheres in Simple Shear Flow by Numerical Simulation." *Fluid Mech.* 155:105-129.
- Gadala-Maria, F. A. 1979. The Rheology of Concentrated Suspensions. PhD thesis, Stanford University, Palo Alto, California.
- Pätzold, R. 1980. "Die Abhängigkeit des Fließverhaltens konzentrierter Kugelsuspensionen von der Strömungsform: Ein Vergleich der Viskosität in Scher- und Dehnströmungen." *Rheol. Acta.* 19:322-344.
- Rutgers, R. 1962. "Relative Viscosity of Suspensions of Rigid Spheres in Newtonian Liquids." *Rheol. Acta.* 2:202-210.
- Zick, A., and G. M. Homsy. 1982. "Stokes Flow Through Periodic Arrays of Spheres." *J. Fluid Mech.* 115:13-26.

Distribution

**No. of
Copies**

Offsite

Dennis Wynne
EM-361, Trevion II
U.S. Department of Energy
12800 Middlebrook Road
Germantown, MD 20874

Robert King
Washington Department of Ecology
P.O. Box 47600
Olympia, WA 98594-7600

Donald Temer
Los Alamos National Laboratory
P.O. Box 1663
MS: G740
Los Alamos, NM 87545

Steven Agnew
Los Alamos National Laboratory
P.O. Box 1663
MS: J586
Los Alamos, NM 87545

Phil McGinnis
Oak Ridge National Laboratory
P.O. Box 2008
Oak Ridge, TN 37831-6273

Zane Egan
Oak Ridge National Laboratory
P.O. Box 2008
Oak Ridge, TN 37831-6273

Samuel D. Fink
Bldg. 773-A Rm. B-112
Westinghouse Savannah River Company
P.O. Box 616
Aiken, SC 29802

**No. of
Copies**

Denis Strachan
Argonne National Laboratory
9700 S. Cass Avenue
Argonne, IL 60439

Ed Beahm
Oak Ridge National Laboratory
P.O. Box 2008
Oak Ridge, TN 37831-6223

Steve Conradson
Los Alamos National Laboratory
P.O. Box 1663
MS: D429
Los Alamos, NM 87545

Onsite

3 DOE Richland Operations Office

S. T. Burnum
P. E. Lamont
C. S. Louie

15 Westinghouse Hanford Company

J. N. Appel
H. Babad
G. R. Bloom
A. L. Boldt
S. J. Eberlein
K. A. Gasper
M. J. Kupfer
S. L. Lambert
G. T. MacLean
R. M. Orme
I. E. Reep
D. A. Reynolds
B. C. Simpson
J. P. Slougher
D. J. Washenfelder

Distr. 1

56 Pacific Northwest Laboratory

G. S. Anderson
E. G. Baker
D.L. Blanchard
K. P. Brooks
P. J. Bruinsma
B. C. Bunker
N. G. Colton (5)
J. L. Cox
J. Craig Hutton
T. H. Dunning
A. R. Felmy
S. R. Gano
R. L. Gordon
G. L. Graff
N. J. Hess
L. K. Holton (5)
E. A. Jenne
D. E. Kurath
J. P. LaFemina (5)

M. M. Lamoureux
J. Liu
G. J. Lumetta
R. K. Quinn
B. M. Rapko
D. R. Rector
B. A. Reynolds
R. D. Scheele
L. J. Sealock, Jr.
G. J. Sevigny
P. A. Smith
L. Song
D. L. Styrus
L. E. Thomas
J. M. Tingey
A. J. Villegas
M. J. Wagner
Y. Wang
Information Release (7)